Optimizing an ICA-Wavelet Denoising Method for investigating EMGdi Reflexes

ENGR9700 Engineering Thesis Projects

Student name: Tianshu Chu

Student ID: 2103843

Supervisor: Karen Reynolds; Peter Catcheside

Date of Report Submitted: 16/10/2017

School of Computer Science, Engineering, and Mathematics

Faculty of Science and Engineering

Flinders University

This thesis is submitted for the degree of Master of Engineering (Biomedical)

TABLE OF CONTENTS

List of Figures

List of Tables

List of symbols and abbreviations

EMGdi: Diaphragmatic Electromyography

ECG: Electrocardiogram

COPD: Chronic Obstructive Pulmonary Disease

OSAS: Obstructive Sleep Apnoea Syndrome

OSA: Obstructive Sleep Apnoea

RMS: Root Mean Square

EMGgg: Genioglossus Electromyogram

EMGsc: Scalene Electromyogram

ICA: Independent component analysis

PCA: Principal Component Analysis

Db: Daubechies

MSE: Mean Square Error

SNR: Signal-to-Noise ratio

WT: Wavelet Transform

FT: Fourier Transform

DWT: Discrete Wavelet Transform

STFT: Short-Time Fourier Transform

CWT: Continuous Wavelet Transform

NAVA: Neutrally Adjusted Ventilator Assistance

PSD: Power Spectral Density

Declaration

I certify that this thesis does not incorporate without acknowledgement any material previously submitted for a degree or diploma in any university; and that to the best of my knowledge and belief it does not contain any material previously published or written by another person except where due reference is made in the text.

Tianshu CHU

15/10/2017

Acknowledgements

This project was supported by Flinders University. I wish to express my sincere thanks to my project supervisor Dr Karen Reynolds, for providing me with all the continuous support during the entire project with her patience, motivation and immense knowledge.

I also would like to thank to my second supervisor Dr Peter Catcheside, associate professor at Flinders University. I am extremely grateful and indebted to him for providing valuable guidance and encouragement.

In addition, I would like to take this opportunity to express gratitude to Ms Laura Gell, who assisted research application of EMG reflexes. Without her precious assistance it would not be possible to conduct this project.

Further, I am also grateful to Ms Isabella Ellison, the honours student in the AISH sleep research laboratory at Flinders University, for providing the important reflex diaphragm data. Without her clinic data, I am not able to test the filter algorithms.

Besides, my sincere appreciation also goes to the NeuRA group based in UNSW. They provided the intramuscular diaphragm EMG data and EMG data from the catheter. Those data are very useful for the method validation.

Abstract

Diaphragmatic electromyography (EMGdi) signals can be recorded from surface electrodes placed on the chest wall, intra-muscular electrodes placed directly into the muscle, or via multi-channel intra-oesophageal electrode recordings. EMGdi recordings contain detailed information regarding the central neural drive to breathe and mechanoreflex mediated changes in muscle electrical activity over the course of each breath, and well known to operate in other respiratory modulated pump muscles such as the scalene, and upper airway dilator muscles such as the genioglossus. Thus, assessment of EMGdi activity can help with the assessment of overall neural drive to breathe, and in exploring respiratory pathological mechanisms and respiratory reflex mechanisms. Although somewhat invasive, intra-oesphageal recordings provide high quality EMGdi recordings without contamination by intercostal muscle activity or the attendant risks of pneumothorax and infection associated with intramuscular recordings. However, raw EMGdi signals are heavily contaminated by ECG artefact, particularly when recorded via an intra-osephageal catheter. Thus, reliable assessment of respiratory related intra-esophageal EMGdi requires removal of ECG interference. Conventional methods for ECG denoising of EMGdi predominantly rely on simplistic ECG blanking methods that ignore EMGdi periods containing ECG artefact, or substitute artefact periods with delayed EMGdi recorded a few hundred milliseconds earlier within the respiratory cycle. Whilst these methods are adequate for assessing overall tonic and peak inspiratory levels of EMGdi activity (e.g. from rectified and moving averaged EMGdi after ECG blanking), they are not appropriate for examining within breath reflex changes in inspiratory activity in response to within-breath changes in inspiratory loads, such as mid-inspiratory occlusion. Examination of these reflexes requires signal averaging of raw rectified EMG over many replicated stimuli in order to sufficiently improve signal-to-noise to discern small EMG changes associated with these reflexes. Given that conventional ECG blanking methods destroy large segments of underlying EMGdi activity, signal averaging methods cannot reliably be applied. Averaging of raw unfiltered EMGdi inevitably remains

heavily contaminated with ECG. Consequently, meaningful examination of EMGdi reflex responses to mid-inspiratory occlusion has not previously been possible. Recently described ECG filtering methods offer significant promise, but have yet to be applied to examine EMGdi reflex responses. The purpose of the work described in this thesis was to apply newly described EMGdi filtering methods to test, for the first time, if this new approach can allow for assessment of EMGdi reflex responses to mid-inspiratory occlusion.

Chapter 1. Introduction

1.1 Overview

The diaphragm is the main inspiratory muscle (Figure 1). Electromyographic recordings obtained from the diaphragm are non-stationary bioelectrical signals produced by depolarisation and repolarisation of muscle motor units in the vicinity of the recording electrodes. Thus, EMG recordings allow for a detailed assessment of the motor control of respiration. Assessment of EMGdi activity can be potentially very useful for investigating respiratory pathological mechanisms, respiratory reflex mechanisms and investigating better treatment methods in a range of pulmonary diseases such as diaphragmatic fatigue, chronic obstructive pulmonary disease (COPD) and obstructive sleep apnea syndrome (OSAS)(Luo 2009). EMGdi recordings are thus an attractive method for research into diaphragm pathology, and has become an active topic in recent years to monitor insufficient/abnormal muscle activity. Raw EMGdi signals can be obtained via an esophageal catheter, invasive intra-muscular electrodes, or surface electrodes (Zhan, Yeung & Yang 2010). EMGdi signals obtained from esophageal electrodes is usually heavily contaminated by non-respiratory signal "noise" such as ECG, motion artefacts, and esophageal peristalsis. The heaviest interference is ECG artefact, which has a major impact on breath-by-breath measures such as Root Mean Square (RMS), peak inspiratory activity, and EMG reflex assessment via application of signal averaging techniques. This, reliable timing and algorithm based assessment of EMGdi activity requires good cardiac artefact filtering methods. ECG interference displays two main characteristics: in the time domain, the amplitude of the ECG interference is typically much higher than the amplitude of the EMGdi signal; in the frequency domain, the spectrum of ECG artefact partially overlaps with the spectrum of EMGdi signal.

Figure 1 Location of Diaphragm (Tan, J 2017)

1.2 Inspiratory EMG reflex responses to inspiratory loads

An important mechanism in disordered breathing in Obstructive Sleep Apnoea (OSA) that controls why a patient with OSA can have periods of stable breathing and periods of obstructed flow limitation is not fully understood. One assumption is muscle activity, and augmented effort/reflex response to flow limitation might be important. Previous research has shown inspiratory muscle reflex activation and suppression responses to sudden airway obstruction in muscles such as the genioglossus and scalene (Eckert et al. 2008). Figure 2 shows a reflex in response to a sudden drop in pressure induced via a facial mask. Reflex suppression and excitation of muscle activity are observed in both the genioglossus and scalene muscles (Eckert et al. 2008). This reflex activity of Genioglossus Electromyogram (EMGgg) and Scalene Electromyogram (EMGsc) has been established using signal averaging of raw rectified EMG that is not contaminated by ECG artefact, averaged over many replicated applications of an externally applied inspiratory load. However, the raw EMGdi signal is badly contaminated by cardiogenic artefact which likely obscures similar expected reflexes responses in EMGdi (Figure 3). Thus, denoising is required to evaluate these reflexes in the EMGdi. However, respiratory research groups currently lack the tools to adequately denoise EMGdi ahead of a range of subsequent EMGdi measurements, and in particular EMG reflexes obscured by ECG artefact in EMGdi.
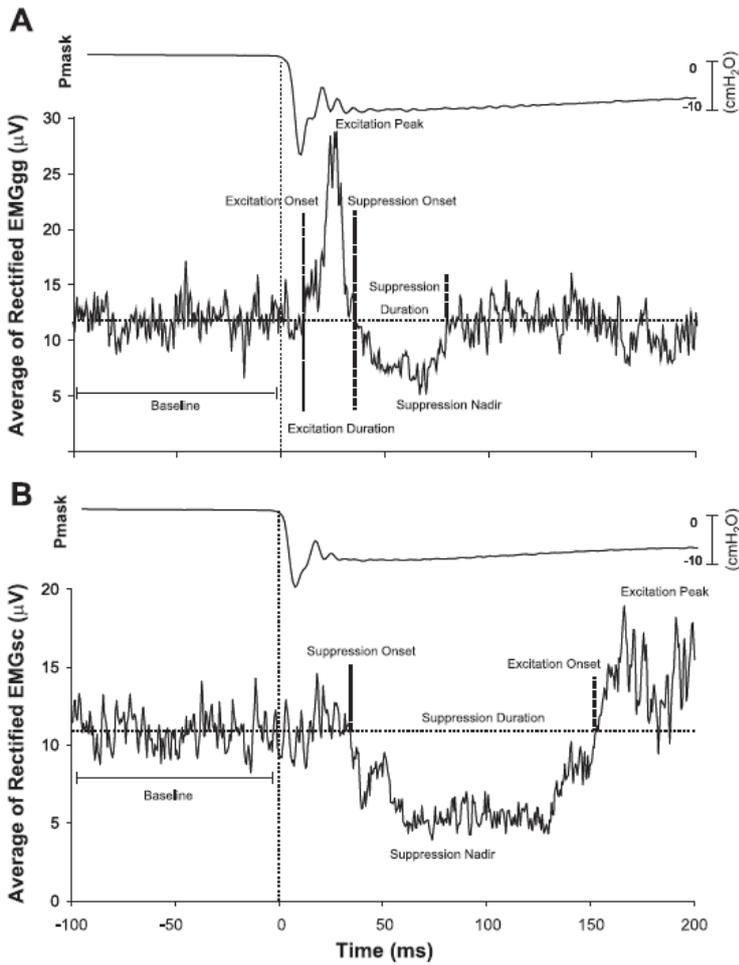
Figure 2 EMGgg and EMGsc reflex responses to mid-inspiratory negative pressure pulse (A: EMGgg reflex; B: EMGsc reflex) (Eckert et al. 2008)
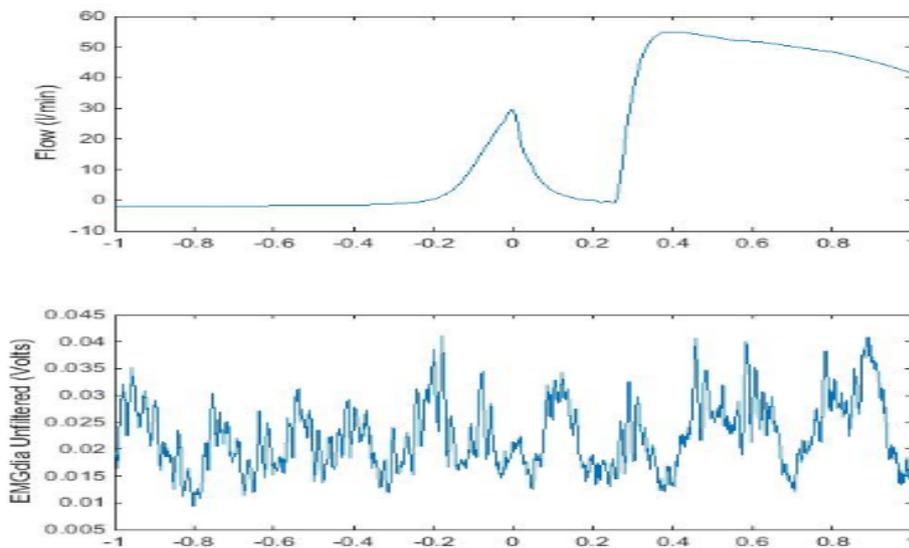
Figure 3 Signal averaged airflow (top) and rectified raw EMGdi (bottom) responses to sudden airway occlusion (N around 100 replicate occlusions)

Prior work demonstrates that the most of the power of ECG signal contamination in EMGdi occurs in a frequency band between 0-70 Hz whilst the most respiratory related EMGdi signal energy is between 25-250 Hz. Thus, there is significant frequency overlap between 25-70 Hz (Wu, Tong & Yang 2016). The main methods currently used for EMGdi noise reduction are simple band-pass filters, gating (e.g. ECG triggered blanking) or subtraction which inevitably contains some residual ECG and destroy a significant component of the real underlying EMGdi signal given overlapping frequencies in ECG and EMGdi.

Traditional hardware or software based "ECG blankers" simply cut and paste a short EMG segment from a nearby part of the breathing cycle. This can effectively clean the signal for the purpose of measuring peak EMG activity during each breath from peak rectified and typically 50-100 msec moving time averaged signal. Simple band-pass filters can also substantially attenuate ECG artefact for this purpose. However, neither method is suitable for assessing short-latency EMG reflex responses to sudden breathing loads on a within-breath time scale, which requires signal averaging of hundreds of replicate trials to obtain the small EMG reflex activity time-locked to stimulus onset. As with genioglossus and scalene, within breath EMG reflex modulation of EMGdi is expected to be small and thus require signal averaging of many replicate responses in order to discern stimulus related reflex activity from non-stimulus activity and noise. However, given that ECG artefact can occur throughout the respiratory cycle, and not necessarily entirely at random given overlap in respiratory and cardiac control, ECG artefact will inevitable regularly obscure the period of interest for assessing EMG reflexes.

1.3 Thesis aim and research direction

Improved methods for denoising EMGdi signals are of significant interest in the field of respiratory and sleep medicine. No previous studies have attempted to examine within-breath EMGdi reflex responses to breathing loads due to the technical problems associated with major contamination by cardiogenic artefact. The aim of this project was to overcome this significant technical problem in order to look at these reflexes in the diaphragm via more sophisticated filtering methods and less destruction of underlying EMG. Understanding short latency muscle reflexes known to operate in other muscles such as

genioglossus and scalene requires better EMGdi filtering than is currently possible with traditional methods such as simple blanking. In the process of the EMGdi signal noise reduction, the effects of noise should be reduced as much as possible and the integrity of the EMGdi signals should be maintained. To denoise the heavily contaminated raw EMGdi signal (Figure 4), several new methods were considered, including a simple subtraction technique, a newly reported wavelet-based adaptive filter, ICA-wavelet filter. The ICA-wavelet approach has conceptual advantages over conventional ECG filtering methods such as band-pass filter and blanking methods, and has the potential to minimise the loss of real signal, and avoiding temporal artefacts introduced with simple ECG blanking. However, this novel filter has yet to be adopted and used routinely in research, and has not previously been tested for examining EMGdi reflexes. The worked described in this thesis aimed to optimize and apply the ICA-wavelet denoising approach to allow for the assessment and comparison of EMGdi compared to EMGgg reflexes expected to be elicited by mid-inspiratory occlusion.
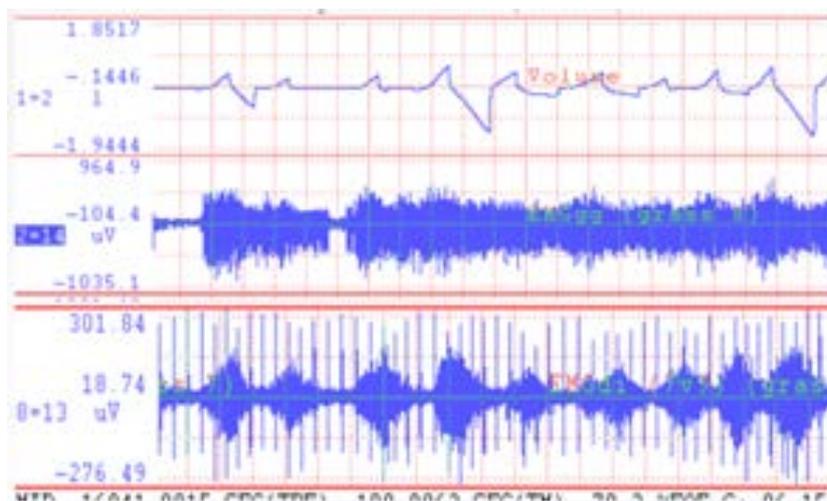
Figure 4 Raw signals (top: Air flow; middle: raw EMGgg signal; bottom: raw EMGdi signal)

1.4 Independent Component Analysis (ICA)

Traditional frequency domain analysis is limited to analyse overlapped spectrum features. Independent component analysis (ICA) is an efficient tool to decompose raw signals into independent components. The basic principle of ICA is to separate the implicit independent source signals from the multi-channel signals (Aapo, Erkki & Juha 2001). According to the classical 'cocktail-party problem', different with Principal Component Analysis (PCA), the

purpose of ICA is not to reduce data variable dimension, but to remove correlations between different components, then find out meaningful physiological or physical signal sources from mixed signals.

Assuming a set of random variables $X(t) = [x_1(t), x_2(t), \dots, x_n(t)]^T$, where $i = (1, 2, \dots, n)$ is the channel number of the observed signal, t is the sample index, it is generated by M mutually independent statistical implicit variables, that is, the source signals $S(t) = [s_1(t), s_2(t), \dots, s_m(t)]^T$ $(m \leq n)$ are mixed linearly through an unknown matrix $A = \begin{bmatrix} a_{11} & \dots & a_{1m} \\ \vdots & \ddots & \vdots \\ a_{n1} & \dots & a_{nm} \end{bmatrix}$:

$$\begin{bmatrix} x_1(t) \\ \vdots \\ x_n(t) \end{bmatrix} = \begin{bmatrix} a_{11} & \dots & a_{1m} \\ \vdots & \ddots & \vdots \\ a_{n1} & \dots & a_{nm} \end{bmatrix} \begin{bmatrix} s_1(t) \\ \vdots \\ s_m(t) \end{bmatrix}$$

To apply ICA validly, source signals should be mutually independent; And the distribution of each source variable should be non-Gaussian (Wang, Kuruoglu & Zhang 2009).

ICA also have limitations: It cannot calculate the source variance index or energy intensity; It is not able to solve the positive and negative sign of the source (Aapo, Erkki & Juha 2001).

1.4.1 FastICA

FastICA is an algorithm to perform Independent component analysis based on fixed point iteration, which allows convergence fast and stable and achieve blind source separation (the procedures are stated in Chapter 3) (Oja & Yuan 2006).

Comparing with other ICA algorithms, FastICA has many advantages (Hyvärinen, Karhunen & Oja 2004). Convergence speed is fast. Unlike gradient algorithm, it is easy to use without step size parameter. Any nonlinear function can be used to find the independent component of any non-Gaussian distribution directly. For other algorithms, the estimation of the probability density function has to be carried out first, so selecting nonlinear is necessary. Its performance can be optimized by selecting the appropriate nonlinear functions. Independent components can be estimated one by one, which reduces the amount of computation in the case that only a few independent components need to be estimated. It is distributed, computationally simple and requires little memory (Hyviirinen 2001).

EMGdi are biomedical signals, which contain sub-Gaussian signals. The FastICA algorithm based on fixed point iteration is a very efficient batch algorithm, so FastICA algorithm is often used in ICA-Wavelet filtering.

In addition, as a linear decomposition method, ICA can separate the source signal as long as the number of collected signal channels is not less than the number of independent source signals. However, for the analyzation of complicated biomedical signals such as EMGdi, the output of decomposition is often incomplete. Nevertheless, wavelet transformation (WT) is efficient for the analysis of non-stable biomedical signals based on its variable timing-window feature. Combining ICA and WT to denoise EMGdi signals can not only overcome the drawbacks of ICA thoroughness but also avoid some drawbacks of wavelet threshold denoising.

1.5 Wavelet analysis

1.5.1 Overview

Wavelet theory is developed on the basis of Fourier transform (FT). Because the Fourier transform analyses the signal completely in the frequency domain, it cannot show the change of the signal at a certain time (Bates 1998). Short-time Fourier transform (STFT) is a tool of time-frequency analysis, which slices the waveform into a number of short segments and performs Fourier analysis on each of these segments (Semmlow & Griffel 2014). The drawback of STFT is that the size of time-window is fixed for all frequencies that can be examined over the chosen time window. The relative duration of high frequency signals is very short, while the duration of low frequency signals is longer. Therefore, we expect a small time window for high frequency signals and a large time window for low frequency signals. Wavelet transform overcomes the deficiency of STFT by allowing for a window function with variable size regions, which is most suited for analysing nonstationary signals such as EMG (Figure 5) (Lu 2013). In the low frequency part, it has higher frequency resolution and lower time resolution, while for high frequencies it has higher time resolution and lower frequency resolution. As a result, WT can more effectively distinguish and extract mutation information from the non-stationary signals, and perform multi-scale analysis by dilation and translation (Semmlow & Griffel 2014). Overall, WT is a time-

frequency, localized and multi-resolution method, which has unique advantages in the processing of clinical non-stationary EMGdi signals.
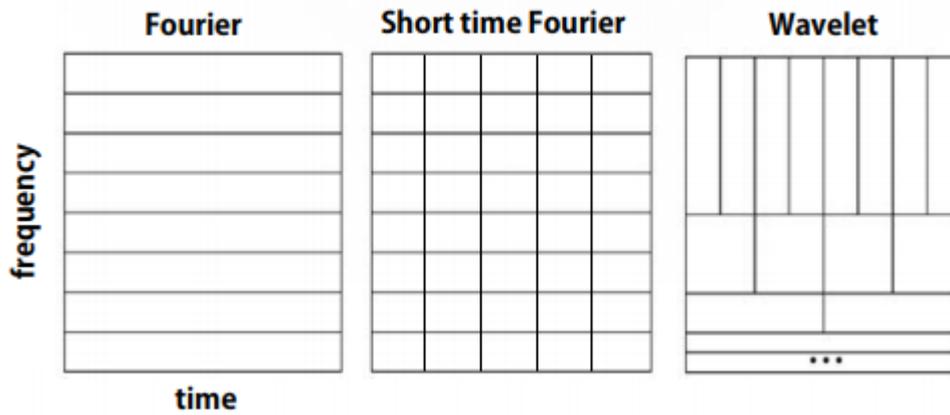
Medical signals such as EMG are usually one-dimensional signals. In one-dimensional wavelet analysis, the Continuous Wavelet Transform (CWT) is defined as the integral transform of the signal $x(t)$ with a family of mother wavelet $\psi_{a,b}(t)$ which is given by (Seljuq, Himayun & Rasheed 2014):

$$W(a,b) = \int_{-\infty}^{\infty} x(t) \frac{1}{\sqrt{|a|}} \psi \left(\frac{t-b}{a} \right) dt$$

After shifting and stretching mother wavelet $\psi_{a,b}(t)$, the wavelet sequence can be obtained, which is given by (Pathak & Singh 2016):

$$\psi_{a,b}(t) = \frac{1}{\sqrt{|a|}} \psi \left(\frac{t-b}{a} \right) \qquad a, b \in R; a \neq 0$$

The Discrete Wavelet Transform (DWT) can be obtained by applying binary discretization of a and b, that is $a = 2^{-j}, b = k2^{-j}, j, k \in Z$ (He, Xing & Yang 2014):

$$W(j,k) = \sum_{j,k} x_{j,k}(t) 2^{-\frac{j}{2}} \psi(\frac{t - 2^j k}{2^j})$$

The discrete wavelet sequence $\psi_{j,k}(t)$ is given by (He, Xing & Yang 2014):

$$\psi_{j,k}(t) = 2^{\frac{1}{2}} \psi(2^j t - k)$$

Where a, b and j, k are dilation and translation factors respectively.

1.5.2 Wavelet basis

Compared to the standard Fourier transform, the wavelet functions in wavelet analysis are not unique, that is, there are a variety of wavelet functions can be chosen from. So the construction and selection of a wavelet basis is a prerequisite for signal analysis and processing. Constructing a new wavelet basis for any specific applications requires a deep theoretical knowledge and research experience of the signals of interest. Basis functions are generally chosen from classic wavelet functions such as Haar, Daubechies (dbN), Biorthogonal (biorNr.Nd) and Coiflet (coifN) (Tan, HR et al. 2007). Table 1 shows a total of 52 wavelet basis which are common to use including 10 Daubechies, 7 Symlets, 5 Coiflet, 15 BiorSplines and 15 ReverseBior. Optimal wavelet basis selection is important in the wavelet denoising process. Current methods of wavelet basis selection have some shortcomings such as large computation and a signal optimal index (He, Xing & Yang 2014). Seljuq, Himayun and Rasheed (2014) point out that performance of Daubechies wavelet basis is best suit for ECG signal denoising based on simulation results. Further, db wavelet of order 9 (db9) is most appropriate in preserving the features of a denoised ECG signal. However, no research has yet concluded what the best suited wavelet basis function is for EMGdi denoising. Previous paper selected wavelet basis based on research experience for EMGdi signals denoising (Wu, Tong & Yang 2016).

Table 1 General Wavelet family (Tan, HR et al. 2007)

Wavelet Family	Wavelet function
Daubechies	db1, db2, db3, db4, db5, db6, db7, db8, db9, db10
Symlets	sym2, sym3, sym4, sym5, sym6, sym7, sym8
Coiflet	coif1, coif2, coif3, coif4, coif5
BiorSplines	bior1.1, bior1.3, bior1.5 bior2.2, bior2.4, bior2.6, bior2.8 bior3.1, bior3.3, bior3.5, bior3.7, bior3.9 bior4.4, bior5.5, bior6.8
ReverseBior	rbio1.1, rbio1.3, rbio1.5 rbio2.2, rbio2.4, rbio2.6, rbio2.8 rbio3.1, rbio3.3, rbio3.5, rbio3.7, rbio3.9 rbio4.4, rbio5.5, rbio6.8

1.5.3 Wavelet decomposition layers

Multi-resolution analysis also called scale analysis. It uses multi-scale property of the orthonormal wavelet basis function to expand signals at different scales (Mallat, Stéphane 1999). The ability of multi-resolution analysis is the main reason of the extensive application of WT (Donoho 1992). A sample 5-layer multi-resolution diagram is shown in Figure 6. The relationship of multi-resolution is: $Y = cA5 + cD5 + cD4 + cD3 + cD2 + cD1$. Multi-resolution analysis only decomposes the low frequency part ($cA1, cA2, cA3, cA4$), aiming to construct 'bandpass' filters with different bandwidths, and therefore requires selection of suitable decomposition layers. ECG signal frequencies are concentrated in the low frequency range (0-70 Hz), where wavelet decomposition usually operates so is ideally suited for decomposing the noisy signal into low frequency components.

Redundant decomposition layers increase computational complexity whilst the insufficient decomposition layers will lead to unobvious denoising effect. Normally, 3 to 5 decomposition layers are sufficient for signal denoising (Wu, Tong & Yang 2016). This thesis decided to decompose noisy EMGdi signal into 5 layers to ensure the denoising effect.
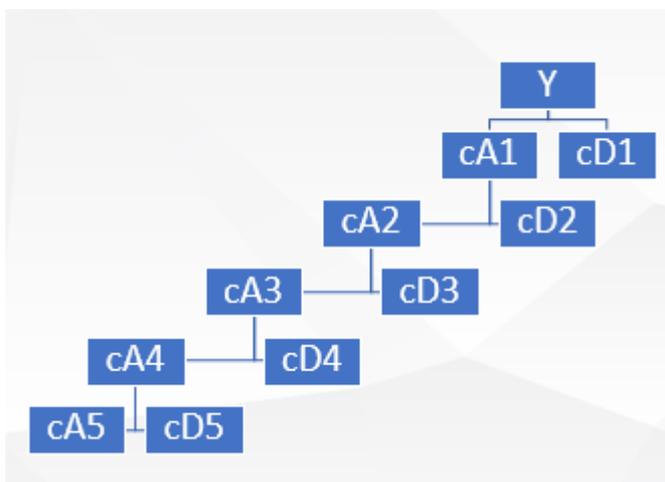
Figure 6 Structure of five-layer multi-resolution analysis

1.5.4 Wavelet threshold

The theoretical foundation of wavelet threshold is based on multi-resolution analysis of WT. When the noisy signal is decomposed by multi-resolution of WT, the discrete detailed coefficients such as $cD5$ and approximate coefficients such as $cA5$ can be obtained after WT

(Figure 6) (Wu, Tong & Yang 2016). Mallat, Stephane and Hwang (1992) proved that the magnitude of the noise's discrete detail signal decreases with the increase of the scale of WT, but the relationship of WT coefficient of useful signal (EMGdi) and the scale is different. Based on this difference, a threshold can be selected to deal with the discrete details of each scale after the WT, followed by the reconstruction of discrete signals (wavelet inverse transformation) to achieve the signal denoising. Traditional threshold functions contain 'hard threshold' function and 'soft threshold' function.

'Hard threshold' function is given by (Carré et al. 1998):

$$\theta(x) = \begin{cases} 0 \ if \ |x| \leq T_j \\ x \ if \ |x| > T_j \end{cases}$$

Where T_j is threshold, x is wavelet coefficient after WT, $\theta(x)$ is wavelet coefficient after threshold selection. 'Hard threshold' sets the wavelet coefficients of which absolute values are less than the threshold to 0, and others remain unchanged.

'Soft threshold' is given by (Deny, Wolf & Bullemer 1988):

$$\theta(x) = \begin{cases} 0 & if \ |x| \leq T_j \\ sgn(x) \cdot |x - T| & if \ |x| > T_j \end{cases}$$

Where T_j is threshold, x is wavelet coefficient after WT, $\theta(x)$ is wavelet coefficient after threshold selection, $sign(x)$ is sign function. 'Soft threshold' means the wavelet coefficients of which absolute values are less than the threshold are set to 0, and other coefficients are compressed to 0.

The threshold value is difficult to be selected, because it should be suitable for each decomposition layer. The quality of the signal and thus signal to noise ratio (SNR) will be reduced with selection of an inappropriate threshold value. A universal threshold is given by (Garg et al. 2010):

$$T = \sigma\sqrt{2logN}$$

Where N is the length of the noisy signal, σ is that signal's standard deviation.

In this thesis, before applying WT, noisy signal was pre-treated by ICA to obtain ECG and EMGdi independent components. Further, this thesis used a novel 'variable threshold'

instead of universal threshold. It requires to adjust threshold settings for different layers with different dataset.

The 'variable threshold' function is defined as (Wu, Tong & Yang 2016):

$$\theta(sig) = \begin{cases} \theta_j(sig) & if \ |\theta_j(sig)| < T[j] \\ 0 & if \ |x| \geq T[j] \end{cases}$$

Where $T[j] = k[j]ave[j]$. $k[j]$ is a weight matrix which can be manually selected depending on different dataset. $ave[j]$ is the average amplitude.

1.6 Performance evaluation methods

Defining how successful a filter is can be hard because of unknown components. Therefore, some evaluation techniques are used to assess ICA-Wavelet performance.

1.6.1 Root Mean Square (RMS)

For n numbers of a discrete distribution, the Root Mean Square of a signal is the square root of mean of the values x_i^2, defined as:

$$x_{RMS} = \sqrt{\frac{1}{n}(\sum_{i=1}^{n} x_i^2)}$$

1.6.2 Signal-to-noise Ratio (SNR)

Refer to Signal-to-noise Ratio definition (Johnson 2006), SNR for this thesis defined as:

$$SNR = \frac{\sigma_{EMGdi}^2}{\sigma_{noise}^2}$$

$$SNR_{dB} = 20 \log_{10}(\frac{EMGdi_{RMS}}{noise_{RMS}})$$

$$SNR_{linear} = 10^{\frac{SNR_{dB}}{20}}$$

Where σ_{EMGdi}^2 is the variance of EMGdi signal, σ_{noise}^2 is the variance of noise value. Theoretically, as the main ECG signal's energy is between 0-70 Hz whilst the main EMG signal's energy is between 25-250 Hz, σ_{EMGdi}^2 can be obtained by producing a 25-250 Hz band pass filter to the denoised signal, followed by calculating the variance. Similarly, the variance of noise σ_{noise}^2 can be obtained via a 50 Hz low pass filter. However, using this

methods only can estimate approximate values because pure EMGdi signals is not able to be direct detected. Thus, other assessments such as median frequency also need to be applied to support EMGdi denoising performance evaluation.

1.6.3 Median frequency

Median frequency can analyse main frequency components of EMGdi signals (Roy, Bonato & Knaflitz 1998). It is a corresponding frequency which divides the entire area of spectrum into half sections (Merletti, Sabbahi & De Luca 1984). The formula is (Wu, Tong & Yang 2016):

$$\int_0^{f_{mid}} PSD(f)df = \int_{f_{mid}}^{f_0} PSD(f)df = \frac{1}{2}\int_0^{f_0} PSD(f)df$$

Where $PSD(f)$ is Power Spectral Density of the EMGdi signal, f is the frequency of EMGdi signal, f_{mid} is the median frequency of EMGdi signal, f_0 is the maximum of frequency of PSD.

If the median frequency of noisy EMGdi signal exhibited in low frequency range (that is, ECG frequency) and the median frequency of denoised signal deviated to a higher value in EMGdi range, it may indicate the ECG noise reduction performance.

Chapter 2. Literature review

2.1 Respiration physiology

This part introduced some common respiratory disease and the relevant analysis using EMGdi.

2.1.1 Diaphragm basics

2.1.1.1 Diaphragmatic fatigue

Diaphragmatic fatigue is associated with failure to maintain a predetermined load of transdiaphragmatic pressure (Pdi) (Roussos & Macklem 1977). Gross et al. (1979) demonstrated the applications and the utilities of EMG and EMGdi in detecting diaphragmatic fatigue via experiments, and evaluated some parameters including esophageal pressures, gastric pressures, pleural pressures, abdominal pressures, transdiaphragmatic pressure (Pdi), bipolar esophageal electrode (EE) and surface electrode (SE) to identify the respiratory muscle fatigue. These findings illustrated the different relative amplitudes of the EMGdi signal when breathing at different levels of Pdi.

In Gross's experiment, the EMGdi signal was passed via two band pass filters. For the power contained in the high frequency band (H), the filter range is 150 Hz to 350 Hz whilst the range of 20 Hz to 46.7 Hz is for the low frequency band (L). Then the ratio of power contained in the H amplitude to the L amplitude in a forced pattern breathing was been calculated to analyse the EMGdi data. Some authors believe that the changes in the H/L ratio of the EMGdi can reflect the diaphragmatic fatigue in the metabolic aspect. Gross's experiment showed a 20% decrease of H/L ratio from start recording so that he concluded the EMGdi signal can detect diaphragmatic fatigue before exhaustion. Levine and Gillen (1987)'s experiment also proved this statement, which gives a fatigue threshold value (20%). They demonstrated that changing features in the power spectral density (PSD) of the EMGdi signal is able to predict the diaphragmatic fatigue (i.e the failure of Pdi maintenance).

It is worth mentioning that the ECG artefact shows a large interference in obtaining H/L ratio. Levine used a high pass filter to remove motion artefact and the cross-correlation technique to remove the ECG artefact.

2.1.2 Central sleep apnea (CSA) & Obstructive sleep apnea (OSA)

Different sleep apnea needs different treatment process so that the differentiation of sleep apneas is important for the subsequent analysis. The theme of article 'Distinguishing obstructive from central sleep apnea events' is to distinguish central sleep apnea (CSA) from Obstructive sleep apnea (OSA) based on the EMGdi and esophageal pressure (Pes) analysis (Luo 2009). In this article, Luo believes EMGdi is an alternative technique to evaluate neural respiratory drive especially within apneic event and compare the airway pressure patterns and respiratory effort via esophageal electrode device other than Pes.

As the 'gold standard' of inspiratory effort evaluation, Pes plays a significant role in analysing sleep apnea. After the experiment, Luo found that both EMGdi and Pes recordings decreased during a hypopnea episode (central sleep apnea events), which leads to the conclusion: The EMGdi signal can differentiate central from OSA.

Luo (2009) avoided ECG interference by measuring the root mean square (RMS) of the EMGdi signal between the QRS complex interval.

2.2 EMGdi Signal and ECG Signal

2.2.1 EMGdi signal

Like other skeletal muscle, activity of nerves innervating the muscle influence muscle activity, via changes in muscle fibre membrane potentials through depolarization and subsequent repolarization processes controlled via the sarcoplasmic reticulum (Calcium switching system). This process will produce electromyographic signal (EMGdi), which can be recorded by electromyography. EMGdi is an indicator which mainly reflects electromyographic activity and functional status of the diaphragm (Beck et al. 1996). EMGdi signals can be recorded via an esophageal catheter which consists several sequential electrode pairs (Beck et al. 1996). The esophageal catheter has multiple-array with alternative electrode configurations. The esophageal catheter used in my project was similar with Beck's device (Figure 7). It contains 10 rings for the basic esophageal electrode. Commercially catheters now in the market such as the one shown in Figure 8. Latest catheters provide better user experience and more functions. For instance, the electrode pairs (stainless steel rings) become narrower and smoother for swallow easier. There are two balloons in the two terminals which can measure respiratory pressures. Refer to the experiment applied to Peter Catcheside in Flinders University (Figure 11), the esophageal electrode catheter will be passed via nose, swallowed into the stomach, and placed down side until all electrode rings can receive signals and show feedback onto the computer. It was difficult to know the exact position of the esophageal catheter inside the body.
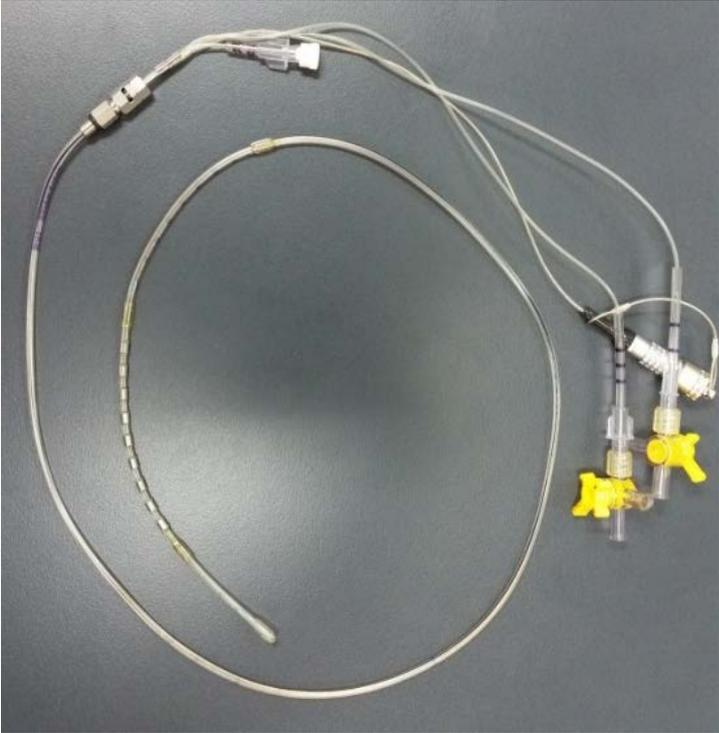
Figure 7 Esophageal catheter used in the Lab

Figure 8 Updated esophageal catheter

Beck's article in 1996 and Wu's research in 2016 provided the similar experimental setup of EMGdi recording (Figure 9 & Figure 10). The esophageal catheter was connected to an electrode configuration adapter, followed by an amplifier assembly, which passband is 0.1 to 1,000 HZ. Wu's device consists 10 electrodes (1 cm long, 2 mm diameter).
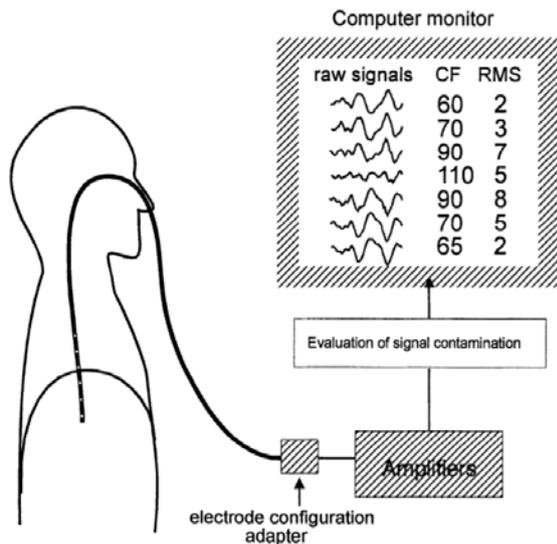
Figure 9 EMGdi signal recording in Bech's article (Beck et al. 1996)
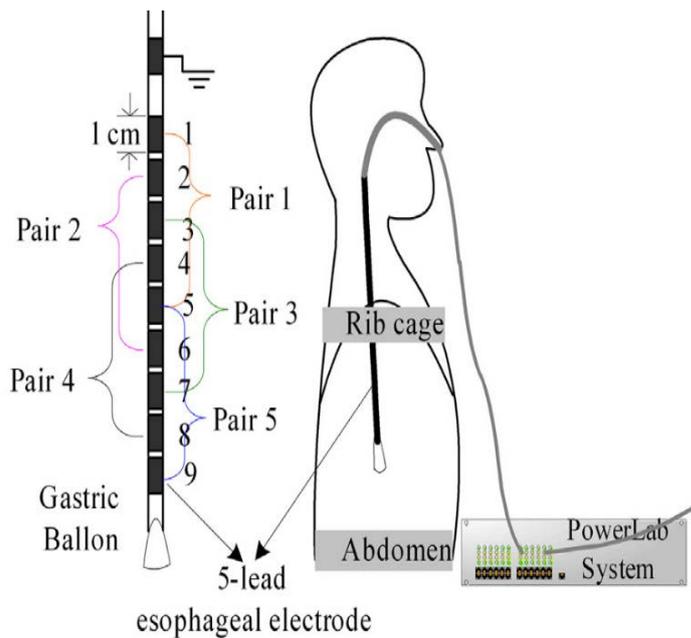
Figure 10 EMGdi signal recording in Wu's article (Wu, Tong & Yang 2016)

Figure 11 EMGdi signal obtaining (Catcheside 2017)

2.2.2 ECG signal

The small electrical current occurs when the heart muscle contracts (Horrobin 1973). This current can be detected by electrodes and reflected by a recording machine which is the electrocardiograph (ECG). The appearance of ECG signal is associated with the cardiac conduction system. This system mainly contains the sinoatrial (SA) node, atrioventricular (AV) node, bundle of His, Purkinje fibres and bundle branches (West 1990). A typical ECG waveform with the names of the deflections and intervals from electrodes on the right arm and left leg (lead II) is drawn in Figure 12 (West 1990). The P wave reflects atrial depolarization (contraction of the atrial muscle fibres). QRS complex reflects ventricular depolarization (start of ventricular muscle contraction). The T wave reflects the repolarization (end of ventricular contraction).
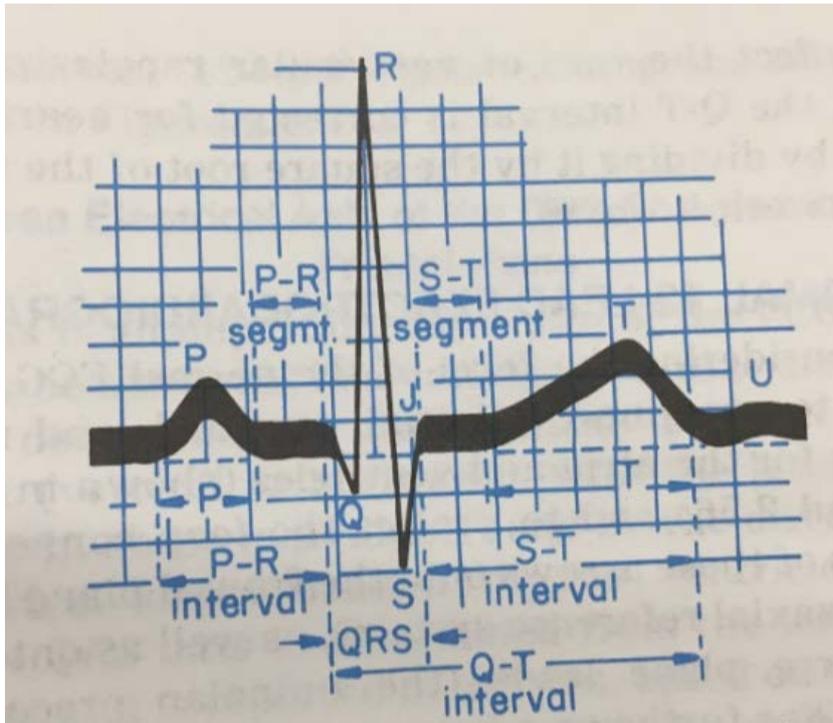
Figure 12 A typical ECG complex with the names of the deflections and intervals (West 1990)

2.3 Signal denoising methods

The evaluation of signal contamination is important to increase the veracity.

2.3.1 Double-subtraction technique

Sinderby et al. (1997) evaluated the concept of 'electrically active region' (EARdi) and effective center (EARdictr) as well as introduced the method of EMGdi signal quality enhancement.

Sinderby's data supports that esophageal electrodes are approximately perpendicular to the fiber direction of a sheet of muscle, where the crural EMGdi comes from. The electrode pairs were placed in 10mm towards EARdictr, which is the best to minimize the influence of muscle to electrode distance-filtering effect and bipolar electrode filtering effect (Sinderby et al. 1997). Therefore, the array of electrode pairs and the signals which come from 10mm towards the EARdictr have the ability to get rid of bipolar electrode filtering and muscle to electrode distance filtering effects. Through the hardware setting, a more accurate EMGdi signal can be obtained. The purpose is to decrease the influence of movement of the EARdictr.

Sinderby also indicated that the EMGdi signals and ECG signals were both amplified during the experiment, and 10 HZ high pass filter was also used. According to Schweitzer et al.'s paper, the high pass filter has been proved not an effective way to analyse the EMGdi signal (Lake, Finucane & Hillman 1999). One benefit of the double-subtraction technique is that it can still receive quality signals when the diaphragm contraction level is low. However, if the subject is suffering neuromuscular abnormalities, the distance between electrode pairs probably will be changed. It is difficult to control the position of EARdictr relevant to the electrode array, which leads to the failure of the experiment and data collection. Moreover, the subtraction method only can be seen as an amplifier which is useful to amplify the EMGdi signal. A separate ECG signal recording, as stated in the article, is not helpful to denoise other EMG channels. It cannot remove the noises such as ECG artifact. More procedures are needed to deal with the EMGdi denoising. Therefore, using hardware to remove the noise and obtain the clean signal seems improper.

2.3.2 Cross-correlation procedure

Levine et al. (1986) used cross-correlation procedure to help remove contaminating ECG noise from the EMGdi signal, compared with other existing approaches. According to Levine's article, ECG frequency spectrum overlaps with the EMGdi signal's power spectral density (PSD).

Previous research employing EMGdi measurements have mainly focused on removing QRS segments of the ECG signal contaminating EMGdi using "gating" methods to detect and remove the QRS segment which is the most obvious contaminating waveform in the ECG spectrum (Bartolo et al. 1996). Figure 13 is an example of using a gating technique which cuts ECG artifacts from the EMGdi signal, replacing either with a zero signal (middle trace) or delayed EMGdi from a non-ECG contaminated part of the signal. However, at high heart rates, the availability of uncontaminated EMGdi is reduced. Moreover, this method destroys part of the real underlying EMGdi signal and introduces temporal artefacts. Another traditional approach has been to use a high pass filter to remove ECG signal. However, high pass filters actually magnified ECG power from direct current-25 HZ to 20 HZ-40 HZ, which has been tested by Schweitzer and colleagues that high-pass filter was not an effective method for denoising EMGdi signal (Levine et al. 1986).
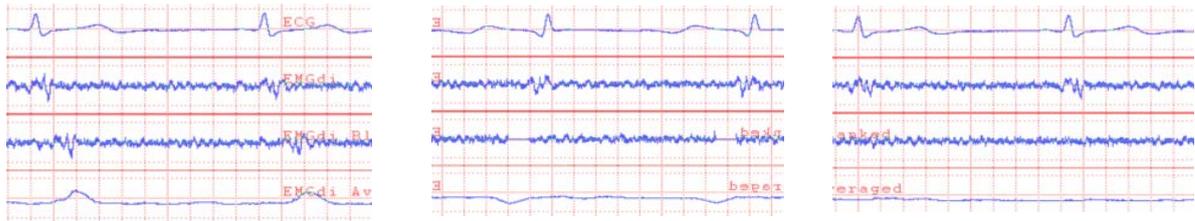
Figure 13 "gating" ECG signal

A further approach is the method that Levine et al. used which is able to detect and subtract ECG components from the EMGdi signals. This approach basically achieved extracting a stationary signal (ECG) from an unstable signal (EMGdi), which includes three procedures. Firstly, a template was identified by the operator during expiration. It depended on the visual determination of the artefact complex. The second step is to determine ECG detection-template correlation and produce Power Spectral Density analysis (PSD). The template is been shifted and correlated to find the correlation coefficients (0.75). Then a program is used to calculate the least-squares linear regression of the EMGdi and judge if the amplitude of EMGdi is larger than 50% of the template amplitude. This step was complex and the accuracy may be questionable. The template should be adjusted in order to match the ECG complex. Thirdly, correlation is used to generate removal-template subtraction. The EMGdi signal can get rid of the modified template.

It is worth mentioning that Levine payed some attention to the influence of ventilation phase, which was a useful to consider. However, as cross-correlation method required selection of a template for analysis, the practicability of this method is potentially limited. The template should be chosen in the inactive EMG interval and close to the ECG waveforms which was still near the contaminated interval of EMGdi. If the subject was dyspnoeic or showing laboured breathing, the effectiveness of this approach may be more limited. Furthermore, arrhythmias or frequent ectopic heart beats make template selection more difficult and negatively impact this method. Levine et al. (1986) only compared PSD analysis results from their gating method, which lacked of the error analysis compared with the original EMGdi signal. Better solutions for obtaining clean EMGdi signals need to be considered.

There is an article particularly compared approaches which described in 4.1.1 and 4.2.1 (Bartolo et al. 1996). The subtraction technique is been set as the "gold standard" to

compare the waveform and the extent error between the original EMGdi signal, the signal processed by gating method and by the subtraction technique.

Bartolo's experiment data were collected from four dogs instead of simulated data. Some EMG variables were applied to support the signal analysis including mean rectified EMG (mrEMG), normalized power (nPWR), median frequency (MF) and mean power frequency (MPF) in this article. The presentation of the outputs was by six bar graphs (Figure 14).
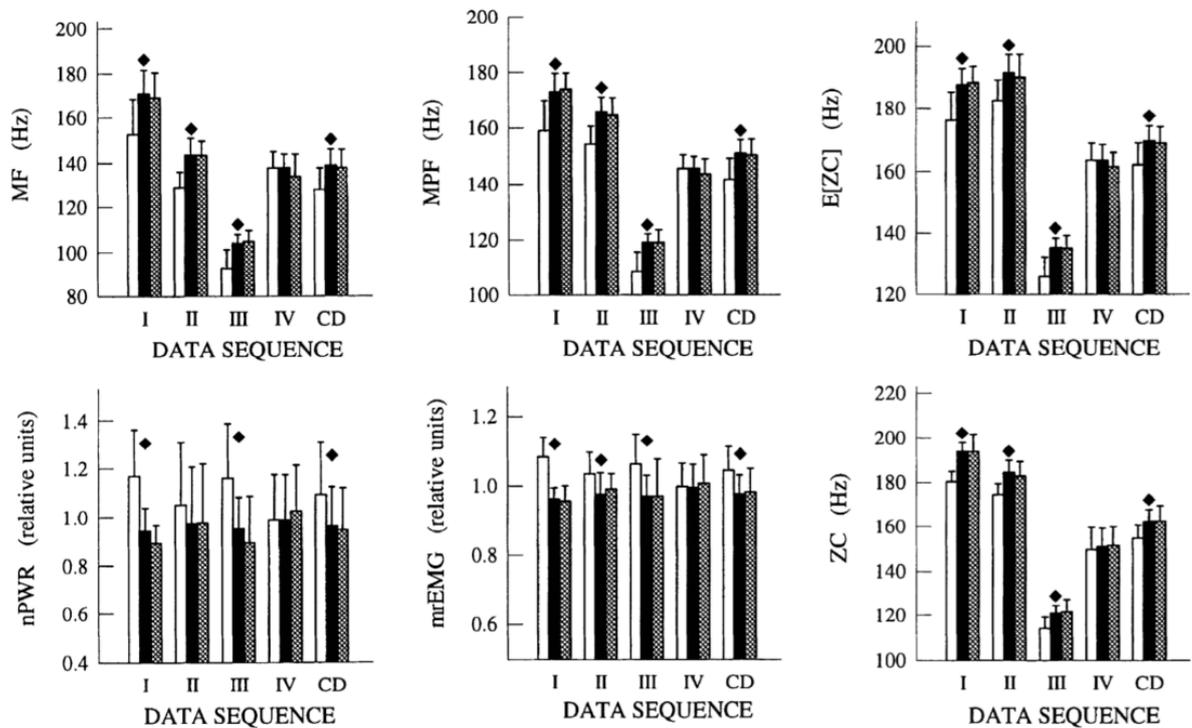
Figure 14 Within-breath analysis refer to data sequence: I-IV represents mean average, SD represents combined data, white bar represents original data, black bar represents the subtracted filter, hatch bar represents the gated filter, MF is median frequency, MPF is power frequency, E[ZC] is expected zero-crossing frequency, nPWR is normalized power, mrEMG is mean rectified EMG, ZC is zero-crossing frequency (Bartolo et al. 1996)

From the bar chart, it can be seen that within the breath, the data derived from gating filter and subtracted filter have not shown a great gap overall whilst they both have great gap from the original data. 'nPWR' and 'mrEMG' value show a drop after both the subtraction and gating filtering, but other values show an increase caused by the subtraction and gating filtering. The EMG-to-ECG power ratio is considered to evaluate the influence of the ECG artifact on the EMGdi signal. For instance, data sequence IV shows very little difference between gating and subtraction, which means the EMG-to-ECG power ratio is large (around

13.3 dB) and the ECG interference is small. Therefore it can be concluded that the optimal position and orientation of the electrodes indeed can minimize the ECG interference.

2.3.3 Wavelet-based adaptive filter

Zhan, Yeung and Yang (2010) 's article focuses on a newer attempt to analyse complex signals such as EMGdi: wavelet analysis. Zhan believes wavelet analysis is useful in multiresolution analysis (MRA), which can be developed as a wavelet-based adaptive filter to denoise the EMGdi signal. The new wavelet-based adaptive filter should be more effective and reference ECG will be unnecessary. The main procedures of denoising EMGdi signals are (Figure 15): 1. Wavelet decomposition 2. Wavelet-based adaptive filter 3. Reconstruction signal.
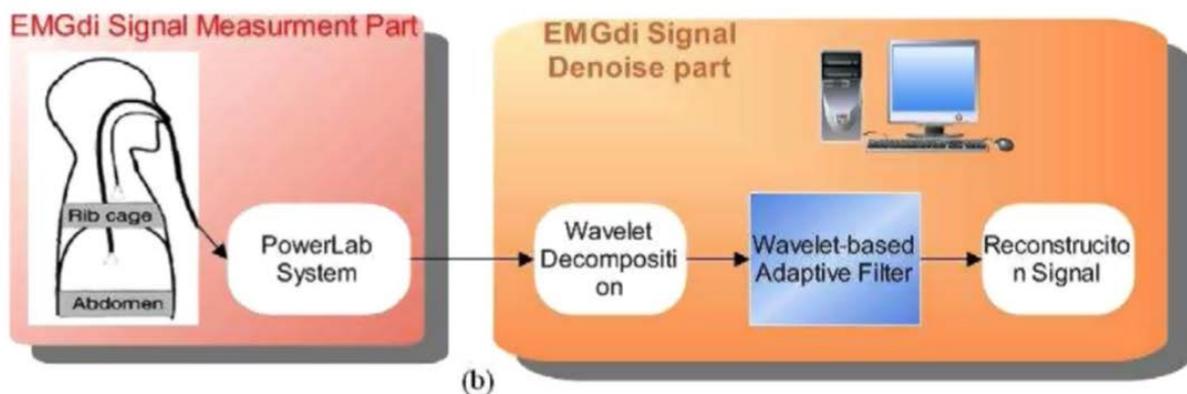
Figure 15 EMGdi signal denoising method (Zhan, Yeung & Yang 2010)
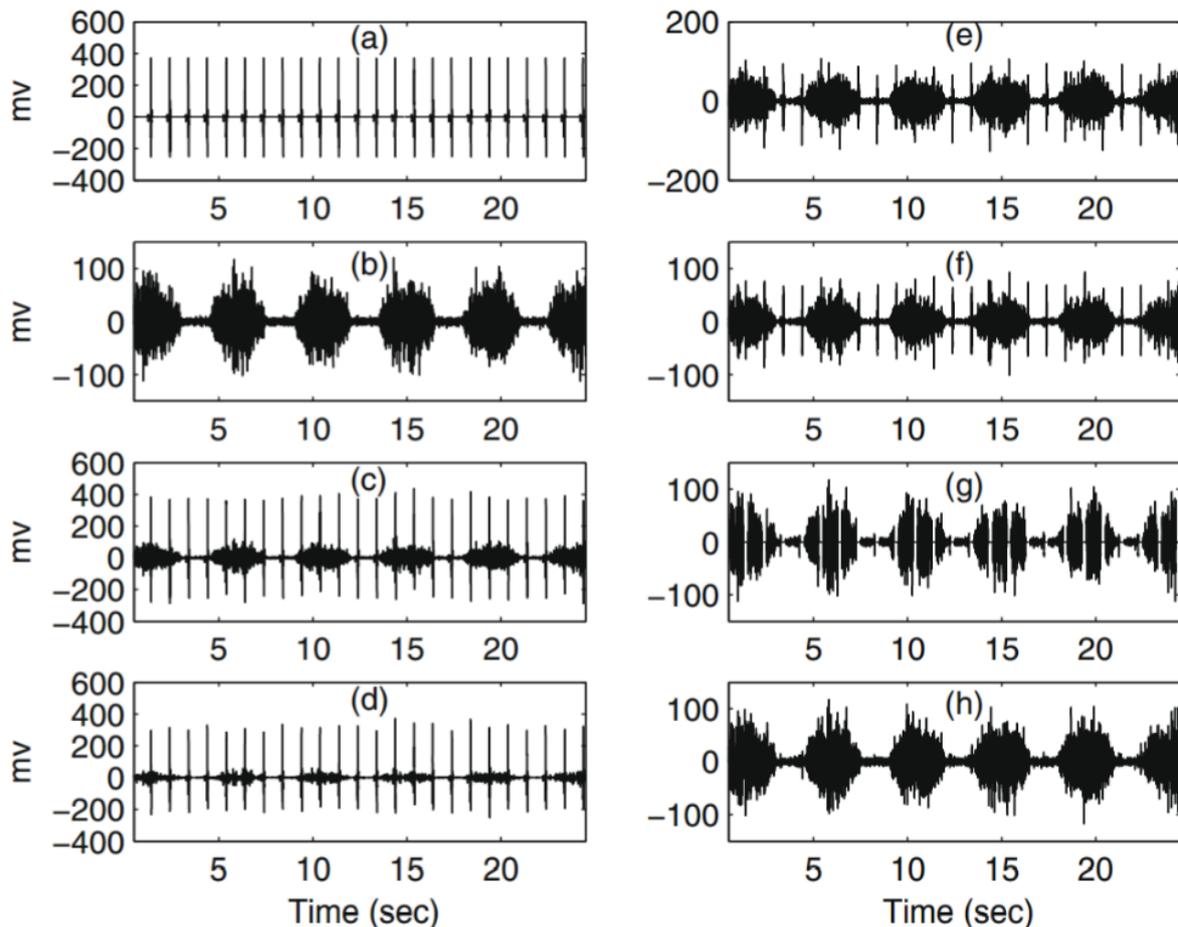
Figure 16 Signals comparison: (a) The ECG artifact signal (b) The pure EMGdi signal (c) The corrupted EMGdi signal (d) Hard thresholding result of EMGdi (e) 'Inverse' hard thresholding result of EMGdi (f) High pass filter result of EMGdi (g) Gating technique result of EMGdi (h) wavelet-based adaptive filter result of EMGdi (Zhan, Yeung & Yang 2010)

Figure 16 shows a summary of simulation example of eight typical signals in Zhan's article. After the comparison, it can be seen that the hard thresholding method will destroy the EMGdi signal while preserve ECG signal. The 'inverse' hard thresholding method preserves the majority of EMGdi signal but ECG artifact also maintain. The high pass filter has been proved not available for ECG interference. The gating method have the capability of removing ECG interference. However, the EMGdi signals which are overlapped with ECG artifact have been removed as well. It can be concluded that so far the wavelet-based adaptive filter can trigger the most similar result with the pure EMGdi signal visually.

It is worth mentioning that some published articles stated that the QRS complex has larger amplitude than EMGdi. After the experiment in Flinders University, it can be seen that EMGdi signal will overlap ECG signal in PSD when the subject produces a deep breath

(Figure 17). It means the amplitude of the QRS complex is not always larger than EMGdi. However, the raw EMGdi signal also contains Gaussian white noise. More investigation need to be applied to the abnormal signals to test the validity of the denoising method.
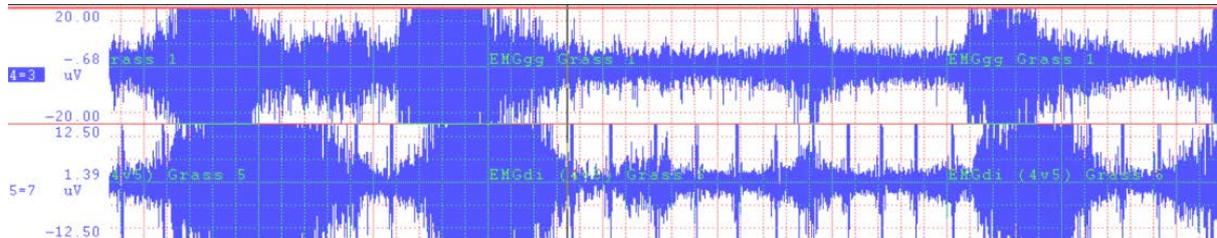
Figure 17 Raw EMGdi signal obtained

The algorithm of the wavelet-based adaptive filter is:

- Obtain wavelet coefficient

- Calculate the average value and adaptive threshold

- Calculate the attenuated decomposition coefficient

- Reconstruct the EMGdi signal
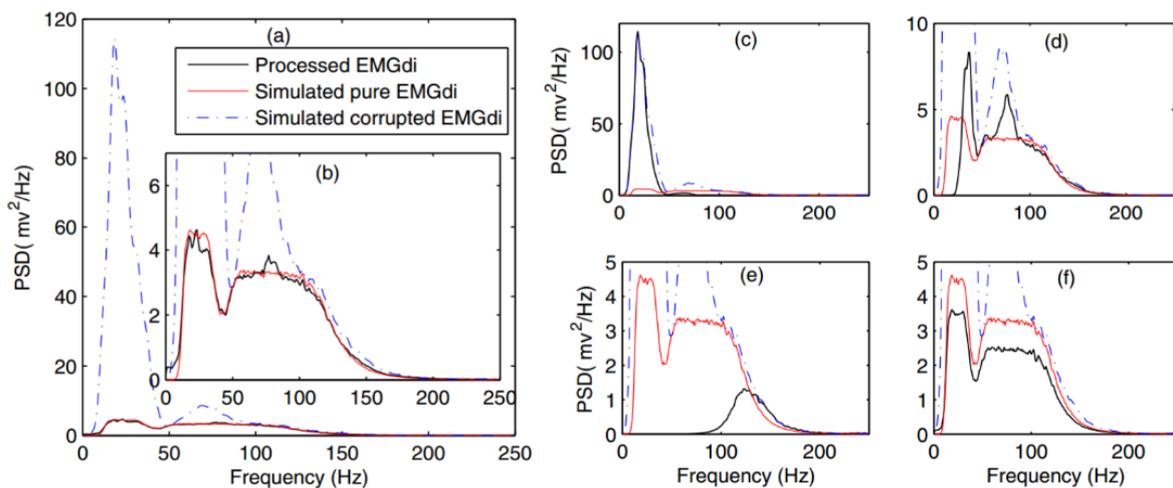
Figure 18 Signals comparison of PSD: (a) Wavelet-based adaptive filter result (b) expanded scale (c) Hard threshold result (d) 'inverse' hard threshold result (e) High pass filter result (f) gating technique result

The article also applied the PSD analysis for different denoising methods. According to PSD results, the wavelet-based adaptive filter has the smallest error of magnitude and shape compared with the pure EMGdi signal. The gating technique result of PSD (Figure 18 (f)) have the same shape but smaller magnitude, which is understandable. PSD analysis is a great idea to identify the filter's quality. Three parameters of PSD analysis are produced in

this article: High to low ratio, total power and centroid frequency. For instance, the EMGdi signal via gating technique processed shows a much lower total power, which means much useful EMGdi signals are also been destroyed. Further parameters can be attempted to obtain more accurate analysis in the near future. Another consideration is that visually we cannot distinguish if the filter has removed all the ECG interference in the overlapped spectrum of EMGdi signal (deep breath area). PSD analysis is not sufficient to prove this problem in the article.

2.3.4 ICA decomposition and wavelet transform

Independent component analysis (ICA) is an emerging EMGdi signal denoising method which has become more and more popular. Wu, Tong and Yang (2016)'s article established the new solution which combined ICA decomposition and wavelet transform to denoise the EMGdi signal, which is updated from wavelet-based adaptive filter.

The algorithm of the traditional ICA used to denoise the surface electromyography includes four main procedures (Wu, Tong & Yang 2016):

- Using ICA to obtain independent components
- Obtain ECG components via a band pass filter
- Recover the contribution of ECG signals
- Subtract the ECG artifacts

However, the traditional ICA contains some shortages. It based on the band pass filter to denoise every independent component of the signal, which has low efficiency on temporal-frequency resolution (Wu, Tong & Yang 2016). It means the denoising capability of traditional ICA is limited. Therefore, Wu indicated FastICA in the article, which used wavelet domain threshold to analyse the independent components instead of traditional band pass filter.

I shall be claiming that the method is under the condition that the hypothesis which ECG artifact owns the largest energy is valid. Therefore the ECG components can be gained fist.
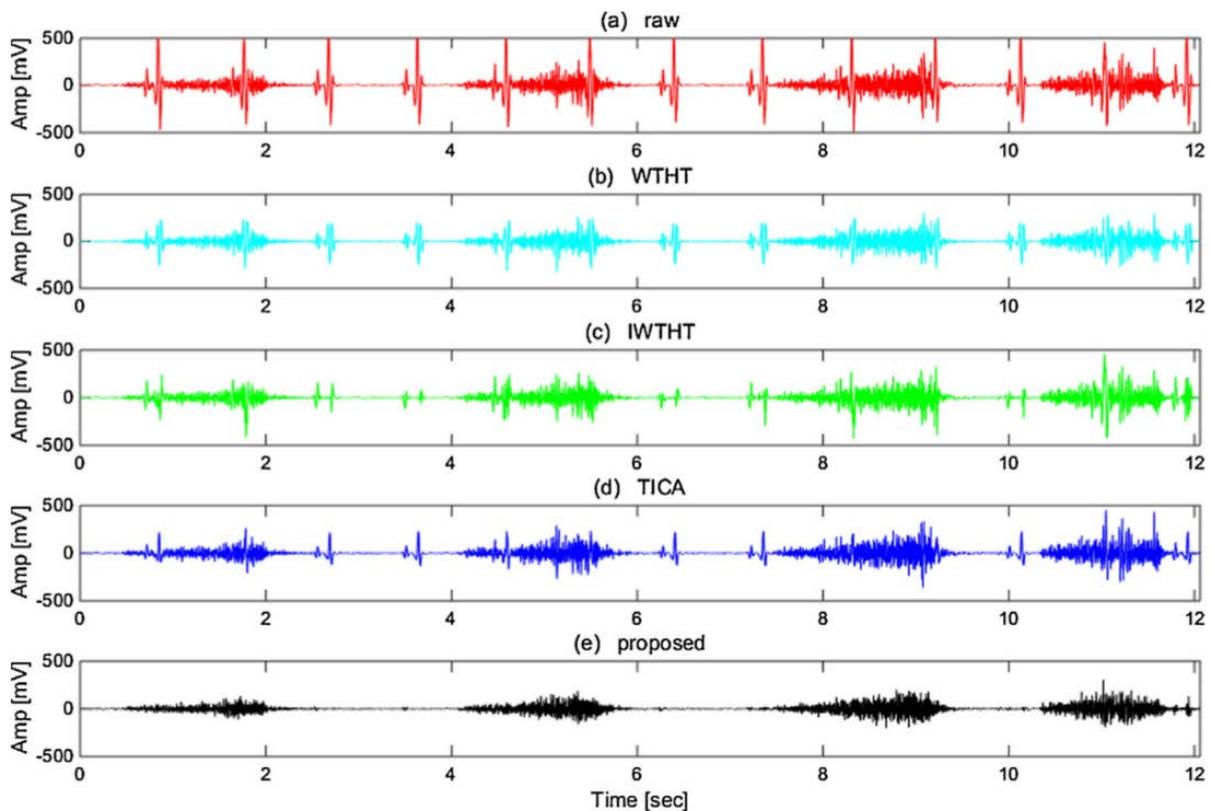
Figure 19 EMGdi signal denoising outputs comparison: (a) raw EMGdi signal (b) hard thresholding filter (c) inverse hard thresholding filter (d) traditional ICA filter (e) ICA—wavelet filter (Wu, Tong & Yang 2016)

Wu compared the different EMGdi signal denoising outputs in his article including WTHT, IWTHT, TICA and ICA—wavelet (Figure 19). Obviously, ICA—wavelet filter is more efficient in removing ECG interference comparing with other filters, especially in the flat interval. As the ECG signals are regularly occurs and the amplitude is larger than every EMGdi signal amplitude especially QRS complex, it can be visually seeing that the ICA-wavelet filter can remove ECG interference in the overlapped spectrum. Nevertheless, the amplitude of the EMGdi signal seems also decreased to a certain extent. Besides, the raw signal in Wu's experiment is simulated whilst the clinical EMGdi signal also contains other interference such as esophageal peristalsis and Gaussian white noise which is more complex. The efficiency that applying to the clinical data needs to be tested.

Wu also compared the EMGdi signal denoising outputs between high pass filter, normalized least mean square (NLMS) filter and ICA—wavelet filter (Figure 20). Visually, all the ECG interference has been removed by ICA—wavelet filter from EMGdi signal without destroying the EMGdi signal.
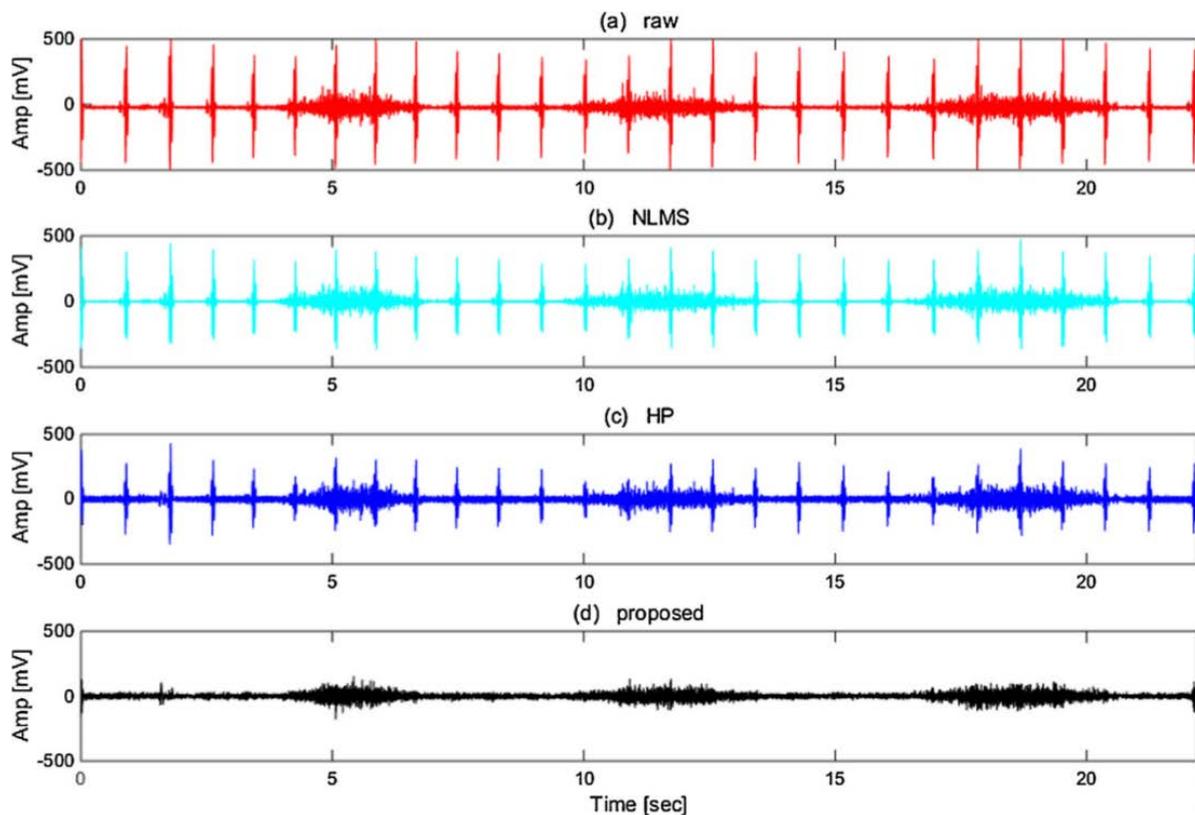
Figure 20 EMGdi signal denoising outputs comparison: (a) Raw EMGdi signal (b) Normalized least mean square filter (c) High pass filter (d) ICA—wavelet filter (Wu, Tong & Yang 2016)

In addition to apply PSD and CF analysis, the average rectified value ratio (ARVR) has also been generated to identify the signal amplitude directly, which is a tool to assess the efficiency of these denoising methods (Figure 21). The ARVR value of ICA—Wavelet filter is close to 1, which means the ECG signal is weak whilst the EMGdi signal is maintained. By calculating ARVR, another evidence shows that the ICA—wavelet filter has the capability to denoise the EMGdi signal to a great extent. Further, more analysis such as mrEMG, nPWR, MF and MPF, as generated in Bartolo's article, can be attempted to test the wavelet-based adaptive filter and the ICA—wavelet filter. Personally, PSD graph and ARVR graph are clear, more intuitive, less messing and easier to draw a conclusion comparing with Bartolo's bar chart.
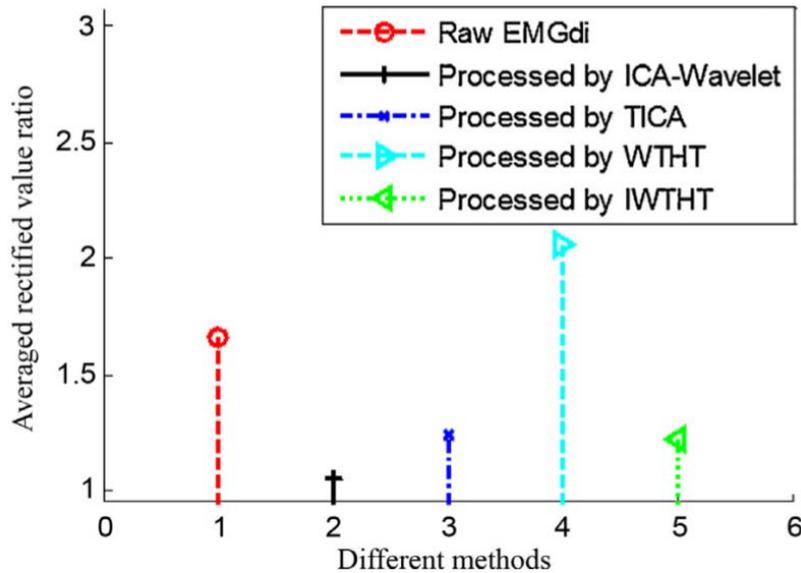
Figure 21 *ARVR comparison (Wu, Tong & Yang 2016)*

So far ICA—wavelet filter is the latest and the most effective approach to remove the ECG interference from the EMGdi signal. We are planning to test this method with Flinders University's clinical data and considering the improvement.

Chapter 3. Theoretical methodology and Experiment details

3.1 Experiment 1: Exploration of ICA-Wavelet algorithm

The implemetation of ICA involves three components including centering data (remove mean), whiteing process (sphere data) and optimizing algorithm to maximize non-Gaussianity of each source (Hyvärinen, Karhunen & Oja 2004). Whitening process aims to decorrelate variables and scale variables so that their variance equal to 1.

The implementation of Wavelet Transform (WT) also contains three parts including wavelet decomposition, wavelet threshold denoising and wavelet reconstruction (Wu, Tong & Yang 2016).
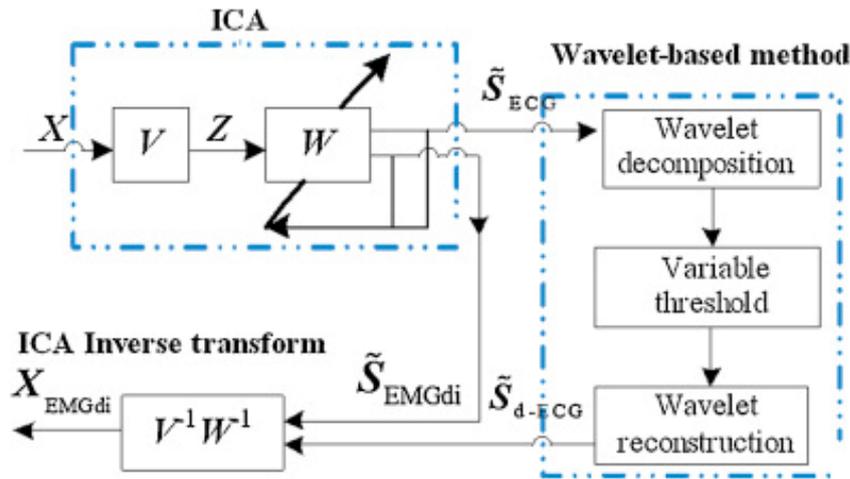
Figure 22 The block chart of ICA-Wavelet algorithm (Wu, Tong & Yang 2016)

Figure 22 shows the block chart of ICA-Wavelet process for the EMGdi noise reduction (Wu, Tong & Yang 2016). The 5×6,474,640 clinical data used in the Experiment 1 comes from a study measured by an honours student in Flinders University. The detail of the block chart is as follows:

1) Firstly, FastICA was applied to the corresponding 5-channel signal $X = [x_1, x_2, x_3 \dots x_m]^t$ to obtain the five independent components, which helps to identify the 'ECG related' components (0-70 Hz) which have larger energy and 'EMG related' components (25-250 Hz) containing lower energy.

2) Secondly, 'EMGdi related' components were extracted and 'ECG related' components $Y = [y_1, y_2, y_3 \dots y_n]^t$ were decomposed into 5 layers by Db1 Wavelet, as 'ECG related' components still contain some weak EMGdi contributions which should be preserved (Figure 6). The fifth layer (cA5 and cD5) should contain the most of the ECG artefact coefficients whilst other layers should contain weak ECG energy. It means 1-4 layers (cD1, cD2, cD3 and cD4) mainly contain relatively lower frequency part of the EMGdi energy.

3) To purify the 'ECG related' components, variable threshold developed by Wu (2016) were used to remove residual ECG energy in each wavelet decomposition levels. Small wavelet coefficients should be ignored as they are dominated by white noise.

4) Then, the purified 'ECG related' components were reconstructed to Y ($\tilde{S}_{d-ECG}$) and the total signal components including 'EMGdi related' part and purified $\tilde{S}_{d-ECG}$ part were reconstructed back to the original signal $V^{-1}W^{-1}$.

3.2 Experiment 2: Performance evaluation

RMS values and median frequencies are calculated to compare the performance of ICA-Wavelet filter in Experiment 1. The spectrum is also plotted to show power features.

3.3 Experiment 3: Optimize the ICA-Wavelet approach

3.3.1 Wavelet basis selection

Not only parameters such as Mean Square Error (MSE), Signal-to-Noise ratio, and correlation coefficient can estimate performance of wavelet basis, but it also requires to retain the valuable features such as peaks of an EMG signal, which shows significant clinical information for early diagnostic purpose (Seljuq, Himayun & Rasheed 2014). This experiment based on the assumption that: performance of dbN wavelet is most appropriate for EMGdi signal; channel one has the best filtering output in Experiment 1.

- First, db1, db4, db5 and db7 are selected respectively to decompose raw signals. Plot filtered Channel 1 signals and compare their features.
- Second, select some more representative orders of Daubechies wavelet family (e.g. db1, db3, db4, db5, db6 and db7) to compare their performance including RMS and median frequency.

Chapter 4. Results of experiments

This chapter shows the results of testing the ICA-Wavelet algorithm and optimising to perform ECG removal on EMGdi. It also involved selecting and testing most effective basis, and verifying removed cardiac frequencies.

4.1 Denoising effect

The sample clinical 5-channel signals are displayed in MATLAB (Figure 23), which contains ECG artefact, other noises and clear peaks of the EMGdi signal. The EMGdi feature (peak blocks) of Channel 4 and Channel 5 are weak. Especially, there are almost all the ECG artefact in Channel 5 with few EMGdi signal. Figure 24 shows the output of the cleaned

signals using ICA-Wavelet filter. Visually, the ICA-Wavelet filter can efficiently remove ECG noise and preserve complete peak details of EMGdi signal in our study. Channel 1, Channel 2 and Channel 3 retain the most accurate features comparing with other two channels which show deficiency on EMGdi blocks in varying degrees visually.
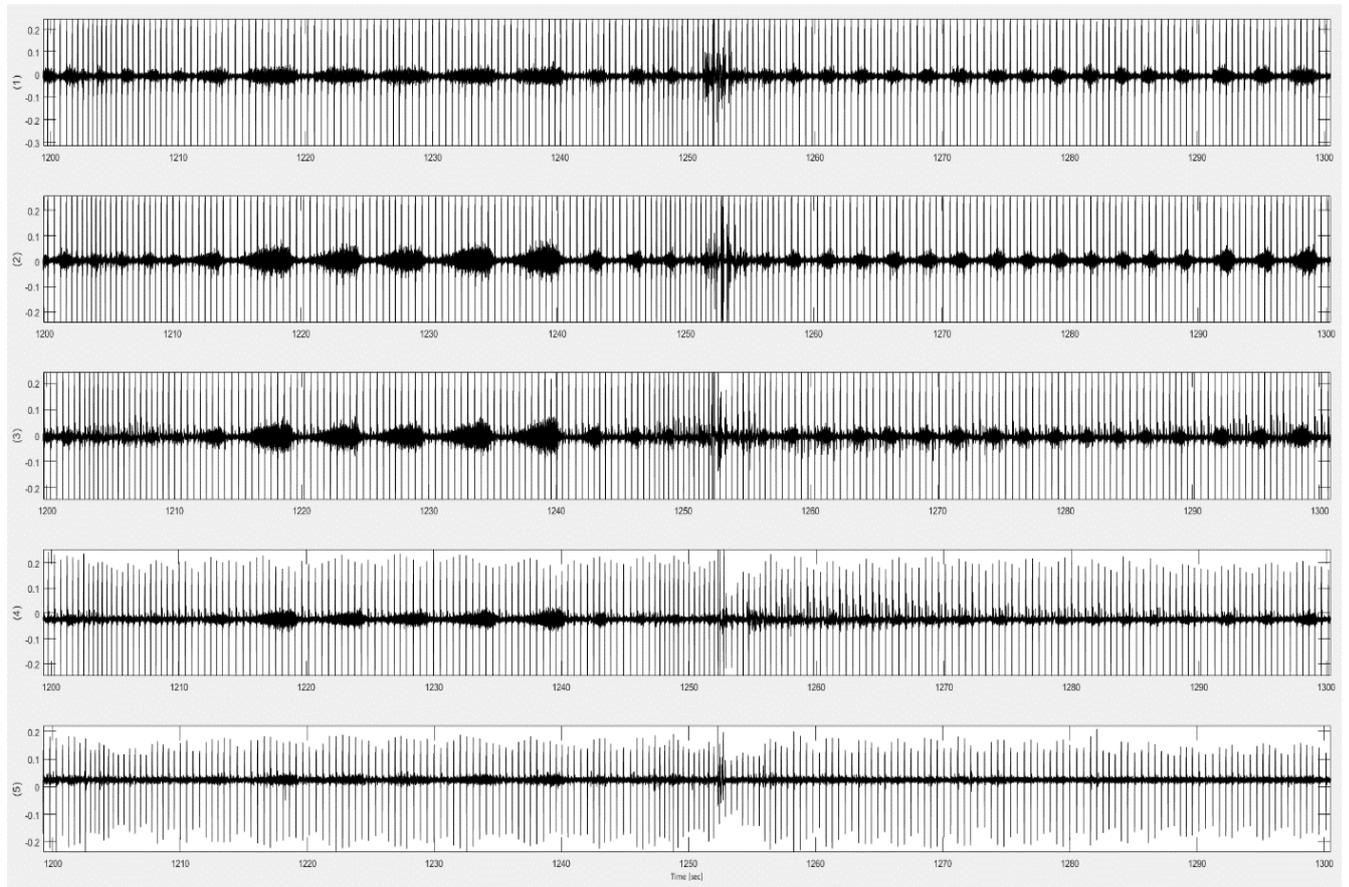
Figure 23 5-Channel raw signals
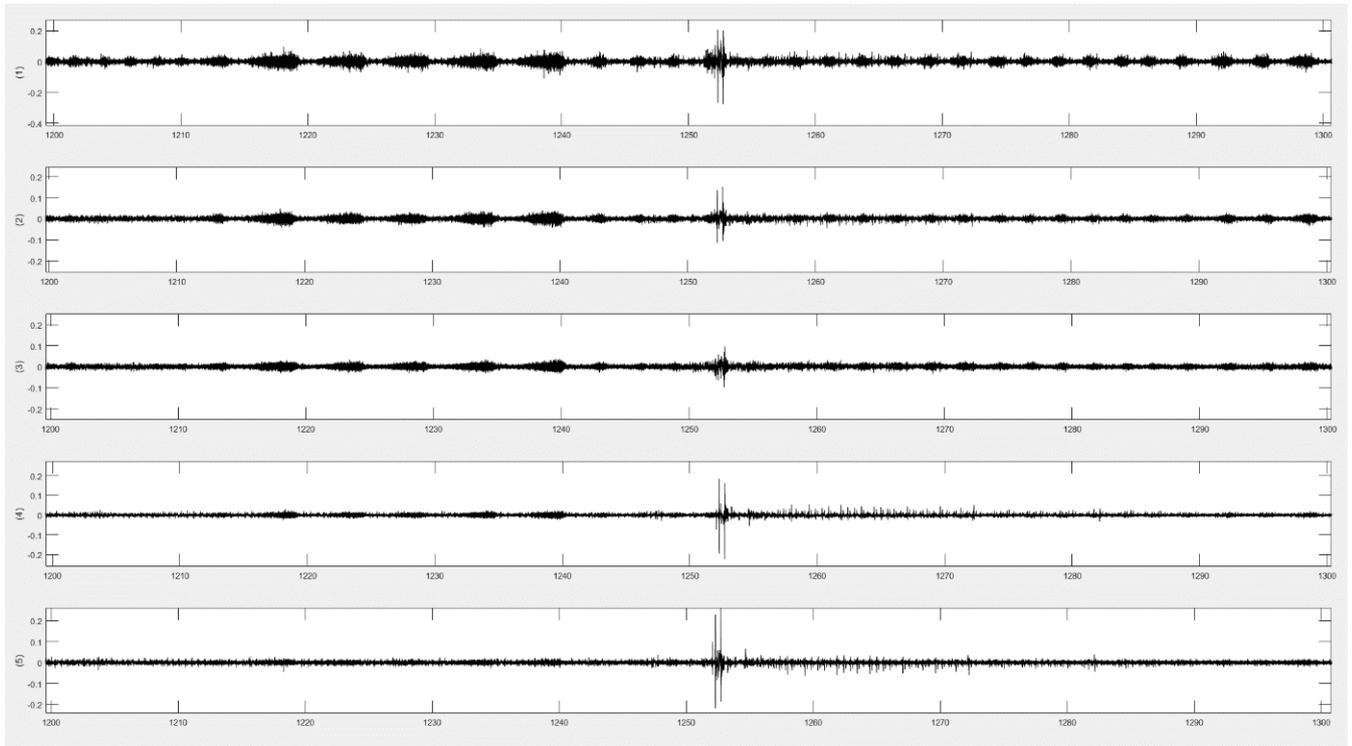
Figure 24 Cleaned 5-channel EMGdi signal

4.2 Performance analysis

The 5-channel RMS values of raw signal and denoised signal in Experiment 1 are shown in Table 2 while the median frequencies are shown in Table 3. The RMS power dramatically decreased from around 133.90 to 23.90 and the median frequency increased from approximately 14.80 to 111.85.

It has been stated in Chapter 1 that the most ECG signal energy is between 0-70 Hz whilst the most EMGdi signal energy is between 25-250 Hz. So if the central frequency can convert from ECG's main frequency range to the EMGdi's frequency range, the ECG component is considered being suppressed.

Median frequency is the frequency value which separate the entire EMGdi signal spectrum area into half equal energy content (Merletti, Sabbahi & De Luca 1984). Table 3 shows the central frequency after ICA-Wavelet filtering has converted from ECG'S main frequency range to the EMGdi's frequency range.

Further, via power spectrum (Figure 25), it can be seen that the amplitude below 50 Hz is much higher than the amplitude at other frequencies in the original signal. It means the energy of ECG signal is much larger than the energy of EMGdi signal in the original signal,

that is, the EMGdi signal is been covered by ECG signal. After the ICA-Wavelet filtering, the amplitude below 50 Hz has an obvious decrease instead of simple removal, which shows ICA-Wavelet filter can effectively decrease ECG artefact in the EMGdi signal. The covered EMGdi signal has emerged from noisy signal. Further, overall power of the signal has dropped and dominated frequency peak around 0-40 Hz cardiac has been significantly reduced.

It's worth mentioning that the median frequency of Channel 4 and Channel 5 are 'unexpected' values. It reflects the atypical clinical collected data (few EMGdi contained), which can be ignored in the future research.

Table 2 RMS values for whole channels

Channel number	RMS (Original)	RMS: (Haar Denoised)
Channel 1	177.9353	34.454
Channel 2	163.4780	21.1514
Channel 3	130.7913	22.4971
Channel 4	110.4564	18.7511
Channel 5	86.8514	22.6370
Mean value	133.9025	23.8981

Table 3 Median frequency for whole channels

Channel number	Fmid (Original)	Fmid: (Haar Denoised)
Channel 1	18.2378	125.0320
Channel 2	20.427	180.6559
Channel 3	21.8387	168.2920
Channel 4	13.4792	42.0074
Channel 5	0	43.2716
Mean value	14.7965	111.8518
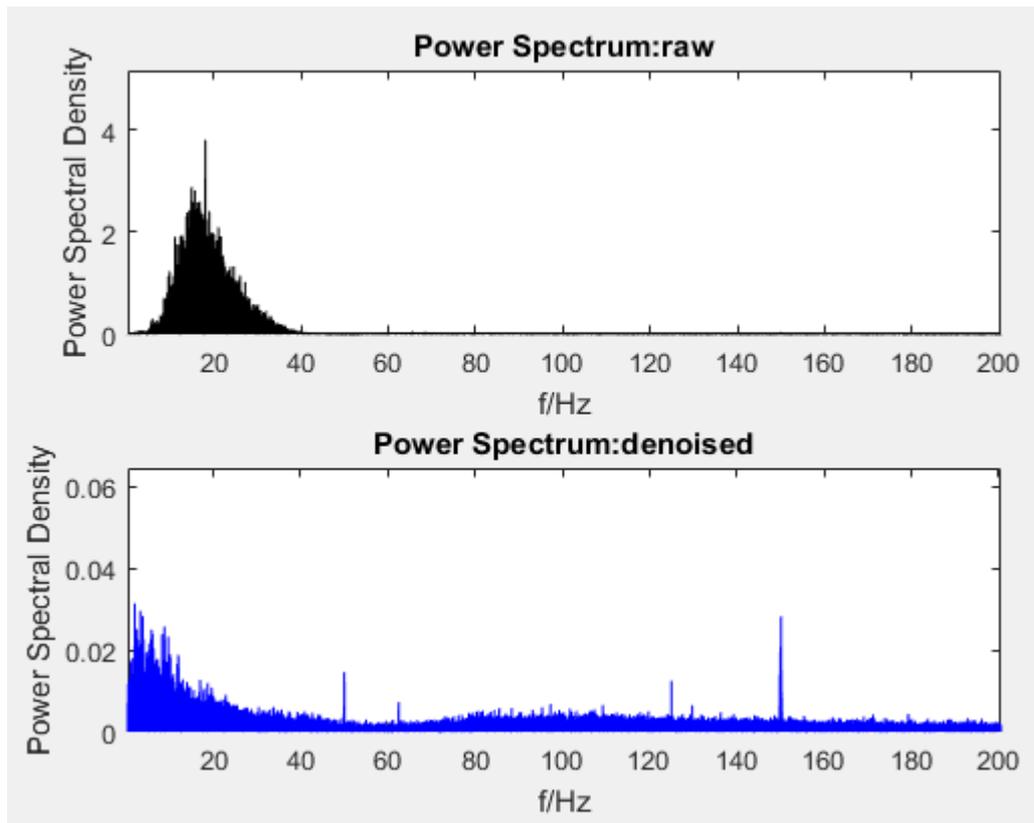
Figure 25 Power spectrum (Channel 1, Haar)

4.3 Wavelet basis comparison

Previous research indicated that low number of db wavelet basis such as db1 is highly localized and the singularity index is small, which can preserve more peak blocks. On the contrary, high number of db wavelet basis such as db8 are highly smooth (Wu, Tong & Yang 2016). After testing all db wavelet family, the output for applying haar, db4, db5 and db7 on the clinical data are shown in Figure 26. There is not much difference on the EMGdi signal visually. Relatively, using haar wavelet basis preserves more 'burrs' via comparison of peak blocks, which has been circled on the figure. The most smooth peak blocks displayed in diagram is with db4 wavelet basis instead of db7, which is different from Wu, Tong and Yang (2016)'s statement. The order of db wavelet basis cannot determine smoothness of the signal in this experiment.

The RMS and median frequency in Table 4 are calculated to compare the performance of different wavelet basis including Haar, db3, db4, db5, db6 and db7. The values are similar and all displayed in a valid range, as stated in 4.2. Hence, ICA-Wavelet filter is robust with db wavelet family. Moreover, Haar wavelet basis has the largest RMS (34.4954) and median

frequency (125.0320), which can be best acceptable in our research to preserve more EMGdi features.
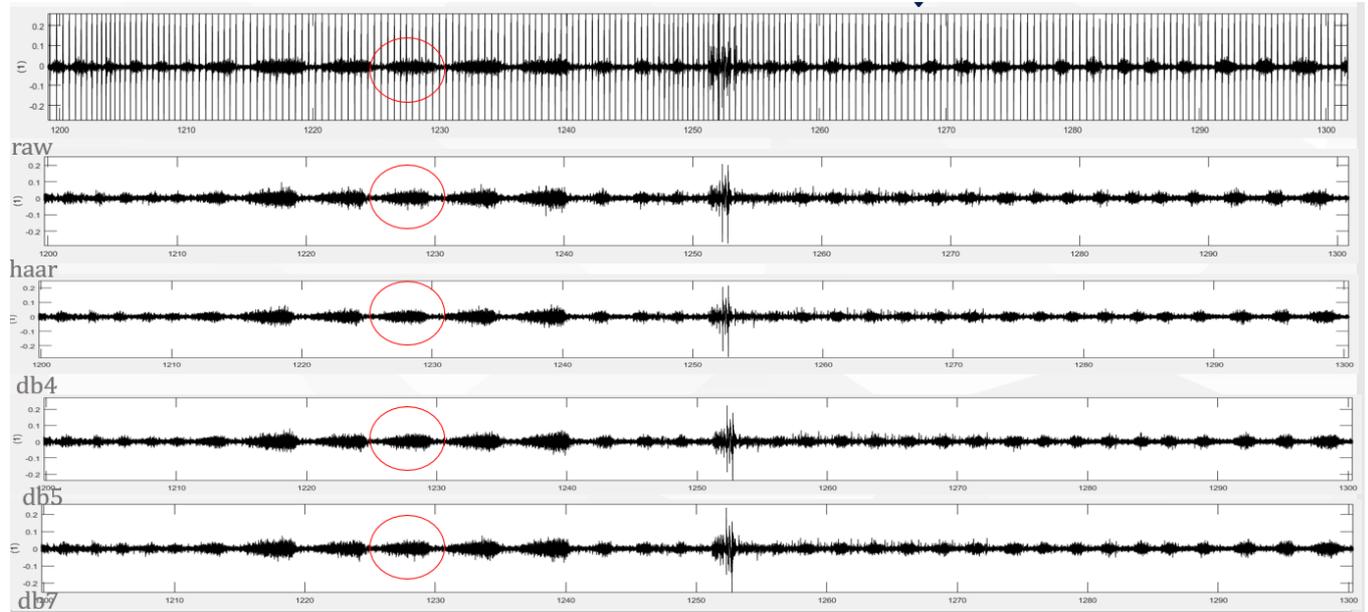
Figure 26 Output comparison of applying Daubechies wavelet family

Table 4 Influence of different wavelet basis on RMS and Median frequency (Channel 1)

	Haar(Db 1)	Db3	db4	db5	db6	db7
RMS	34.4954	33.9653	33.9503	33.8184	33.9993	34.1284
Median frequency	125.0320	121.7785	121.3799	122.7603	120.6966	119.3981

Chapter 5. Discussion

5.1 The family of 'db' wavelet basis

Experiment 3 based on the assumption that performance of dbN wavelet is most appropriate for EMGdi signal so that other wavelet families such as Biorthogonal (biorNr.Nd) and Coiflet (coifN) are not compared in this thesis. This assumption based on previous research's conclusion for ECG signal noise reduction (Seljuq, Himayun & Rasheed 2014), although Zhan, Yeung and Yang (2010) tested that the performances with different

wavelet basis such as Meyer, Symlet and Daubechies are almost the same. However, db4 wavelet basis produces the best performance in their test, while db1 shows the best performance in this thesis.

5.2 Validation of the outputs

It is difficult to evaluate filtering performance and objectively quantify the overlapped cardiac and diaphragm signal. The lost quantity of real EMG signal and the remaining amount of the ECG artefact are unknown by comparing unfiltered and ICA-Wavelet filtered EMGdi signal. EMGgg reflexes is a good comparator to support the results, which provided the significant confidence that filtered EMGdi is preserving expected underlying features. In addition, based on the prior knowledge, visually comparison, investigation of RMS value, mean frequencies/spectrum and other observations also can provide some supports.

5.3 Test with new data

Moreover, a set of neural data was sent by the NeuRA group based in the University of New South Wales from a recent study. The data which measured both intramuscular diaphragm EMG and EMGdi from the catheter is allowed to test ICA-Wavelet filter. Different with previous dataset, raw 'neural' data is messier with abnormal ECG artefact (Figure 28), which should be pre-filtered: a standard 10 Hz high pass filter is selected. The pre-filtered signal is shown in Figure 29 and enlarged Channel 3 is displayed to observe clearer (Figure 30). After ICA-Wavelet filtering, the ECG artefact has been filtered visually (Figure 31).
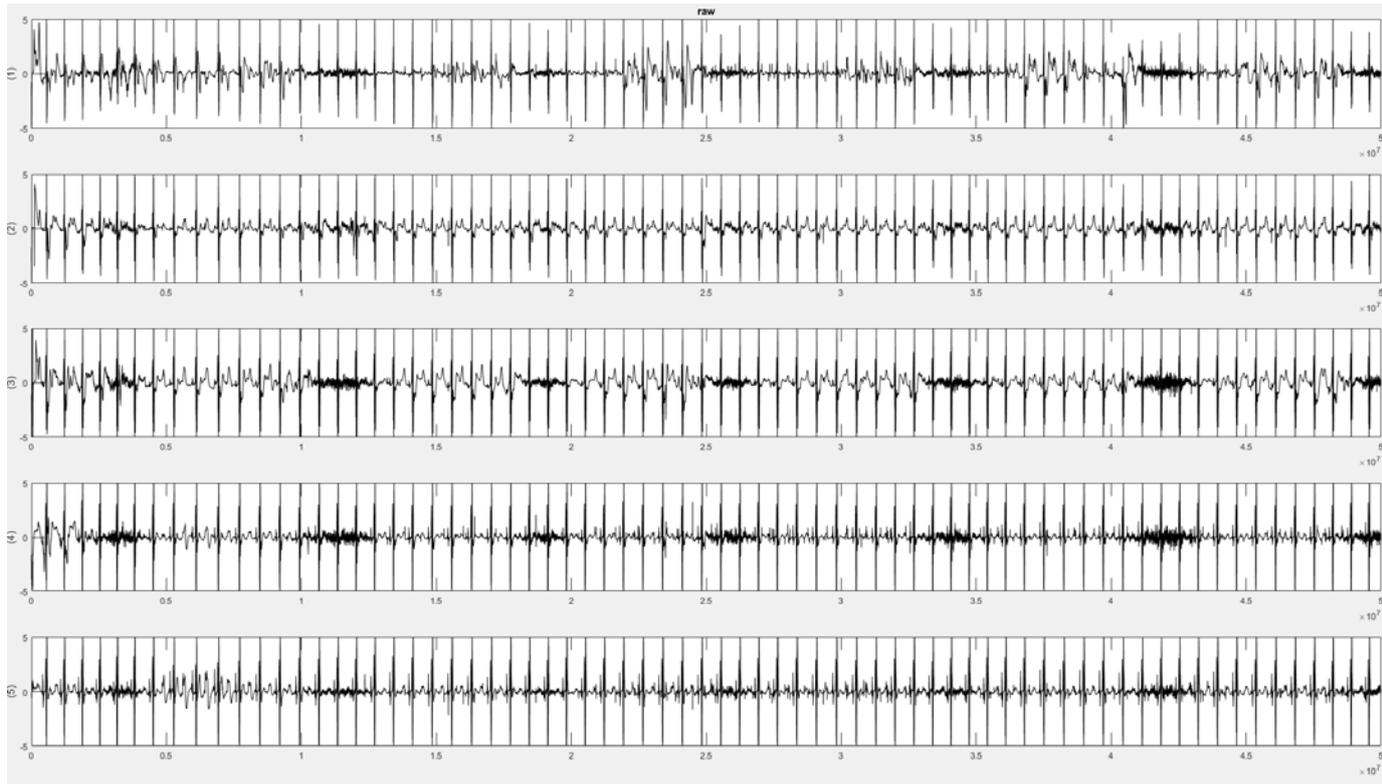
Figure 27 Raw EMGdi signal
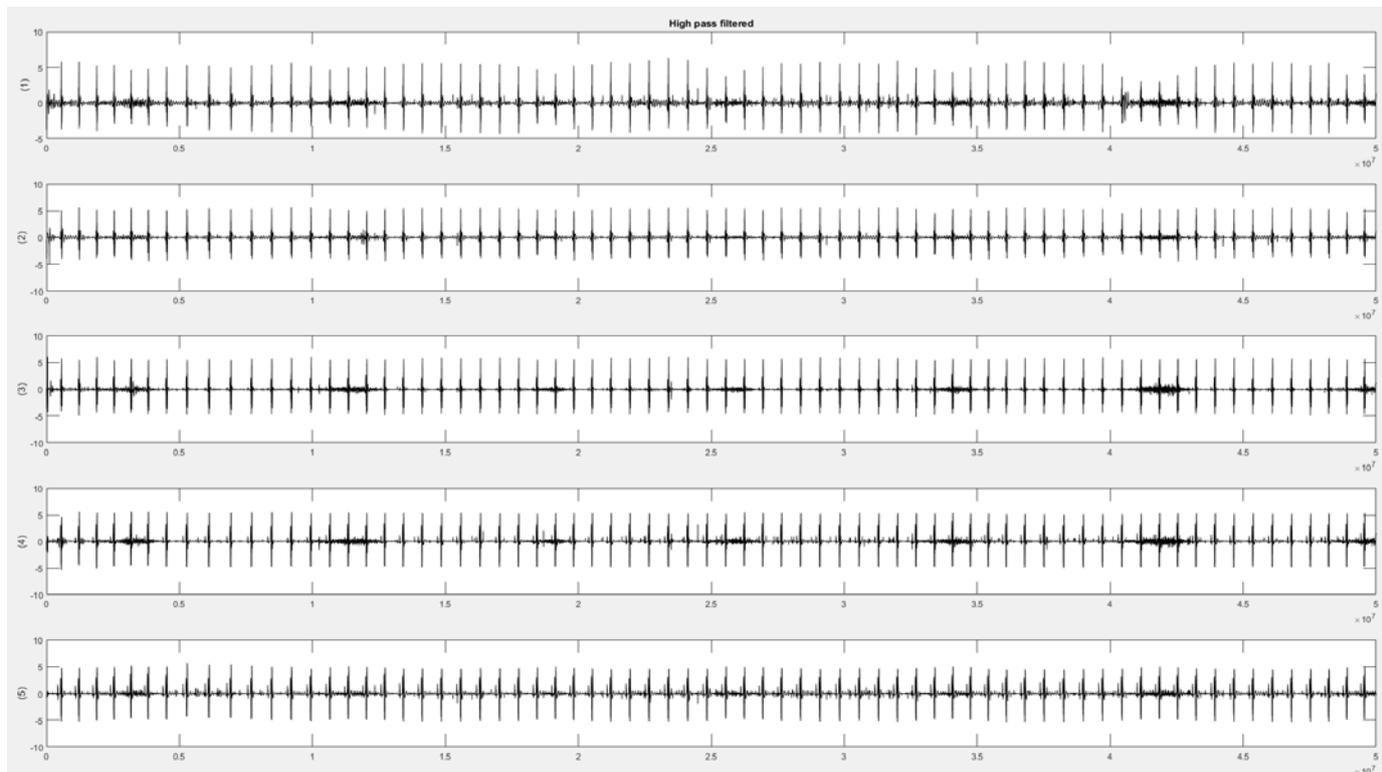

Figure 28 Pre-filtered EMGdi signal
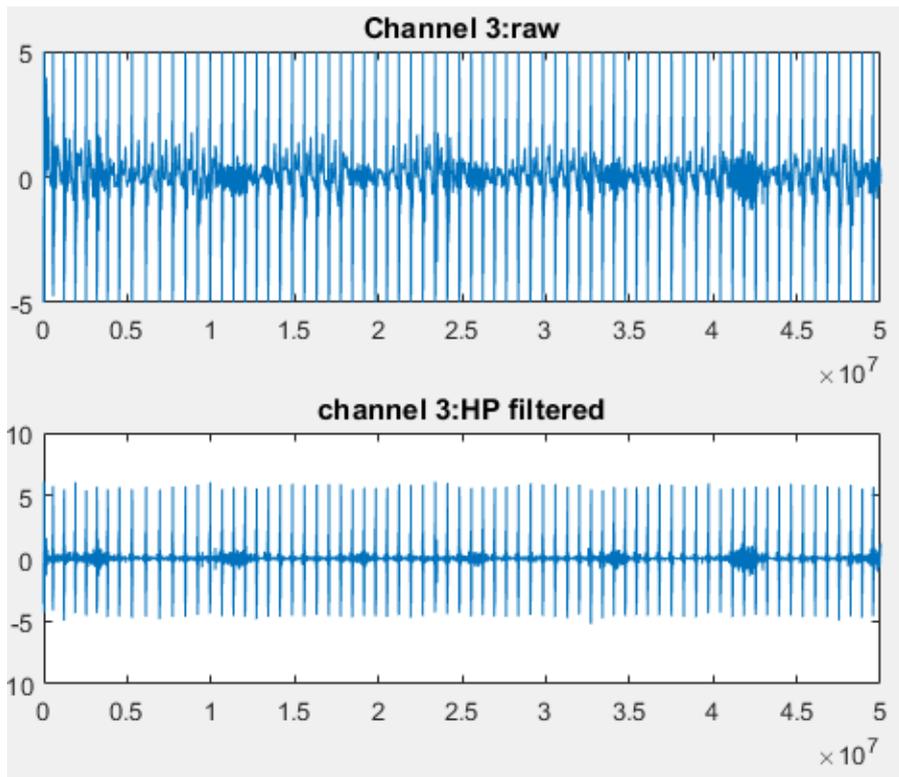
Figure 29 Signal of Channel 3
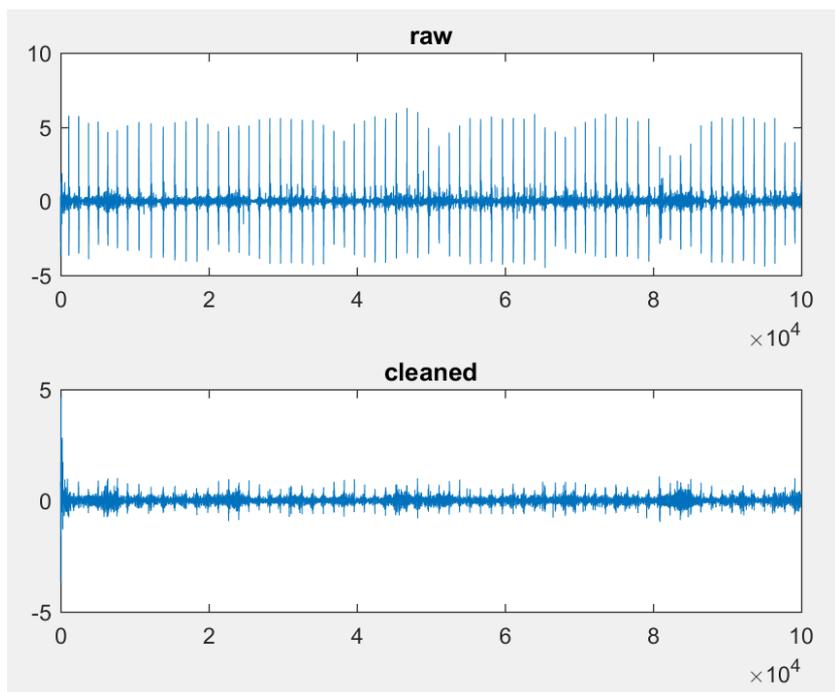
Figure 30 Channel 1 using ICA-Wavelet filter

Chapter 6 Filter application

6.1 Theoretical methodology and Experiment details

An EMGdi reflex response to obstruction could be an important mechanism used by patients with sleep apnea, Neutrally Adjusted Ventilator Assistance (NAVA), and a relatively new mode of mechanical ventilation for critically ill patients, which could influence the disease treatment in the future. Participants were worn a nasal mask which attached to a non-rebreathing valve to control breath (Stadler et al. 2010). The equipment was applied by a solenoid to suddenly cut airflow for about 200ms before airflow was restored within breath and 80 occlusion breaths were applied to each study participant. All of these collected data were time correlated to the point of occlusion and ensembled averaged ± 1 s to give flow and EMG traces. The hypothesis was there would be reflexes in EMGgg and EMGdi. After collecting data, signal averaged airfow, rectified raw EMGdi responses and rectified filtered EMGdi responses to this sudden airway occlusion were plotted to show response features and test the performance of the filter. The EMGgg reflex was also applied to compare with EMGdi responses.

6.2 Results of experiments

The ICA – Wavelet combined algorithm was tested and optimised to perform ECG removal on EMGdi, which involved selecting and testing most effective basis, and verifying removed cardiac frequencies.

Figure 32 and 33 show the output of the application. We cannot observe any expected response in unfiltered EMGdi reflex. Unfiltered EMGdi signal has no capability to expose accurate reflexes because the cardiac signal dominates trace. Comparing with raw signal, filtered EMGdi reveals inspiratory EMGdi activity and expected reflex responses to sudden airway occlusion (Figure 32). The magnitude of unfiltered EMGdi signal is much higher as it was dominated by averaging cardiac peaks. Any short-term reflexes were completely obscured by this cardiac noise. However, the magnitude of filtered EMGdi reflex was lower than raw signal's magnitude. The overall trend of EMGdi reflex was rising in ± 1 seconds with the increased airflow volume. It indicated the ICA-Wavelet filter can be successfully used in the EMGdi reflex study.

Besides, overall pattern of inspiratory EMG activity appears to be similar in the EMGgg and EMGdi (Figure 33). Brief EMGgg reflex activation appeared at the onset of occlusion, assuming more prolonged EMGdi reflex are suppressed. The red arrow on the figure shows the first peak airflow volume occurred at averaging 0 second point which reflected the sudden airflow blocking. The response of EMGdi and EMGgg both increased during $-1\sim0$ sec period. The airflow was then restored and airflow volume decreased until approximately 0.25 sec, which was highlighted in yellow arrow. The EMGdi reflex during this period also decreased same with airflow trend whilst EMGgg reflex kept rising. Then, after a deep inspirary, the airflow decreased gradually. The EMGgg reflex had the same trend with the airflow, but EMGdi reflex still increased a bit.
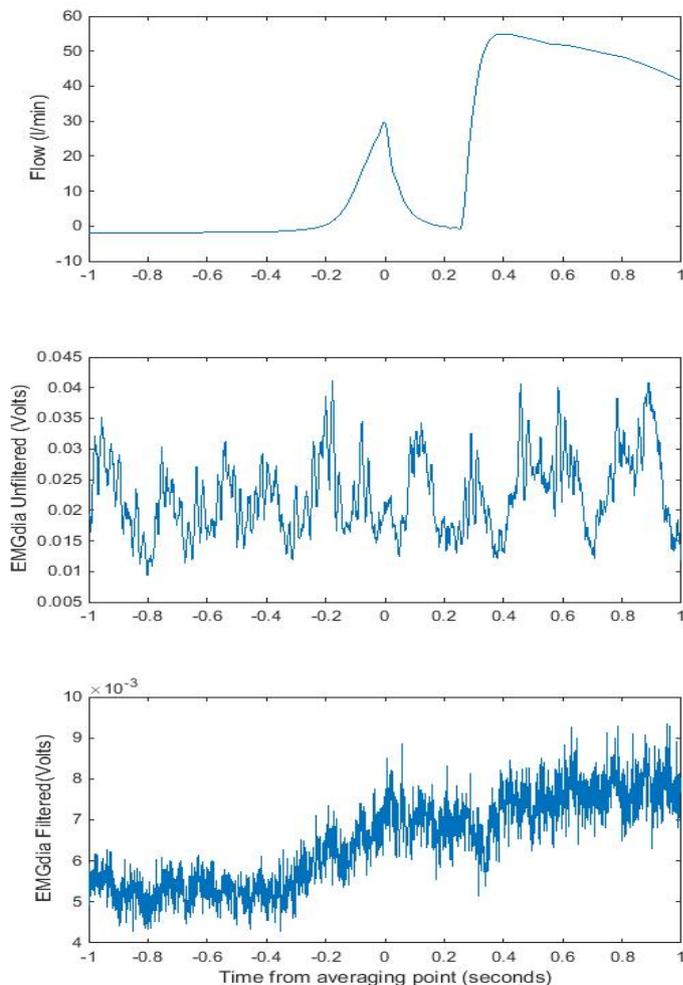
Figure 31 Raw and cleaned EMGdi reflexes elicited by sudden airway occlusion
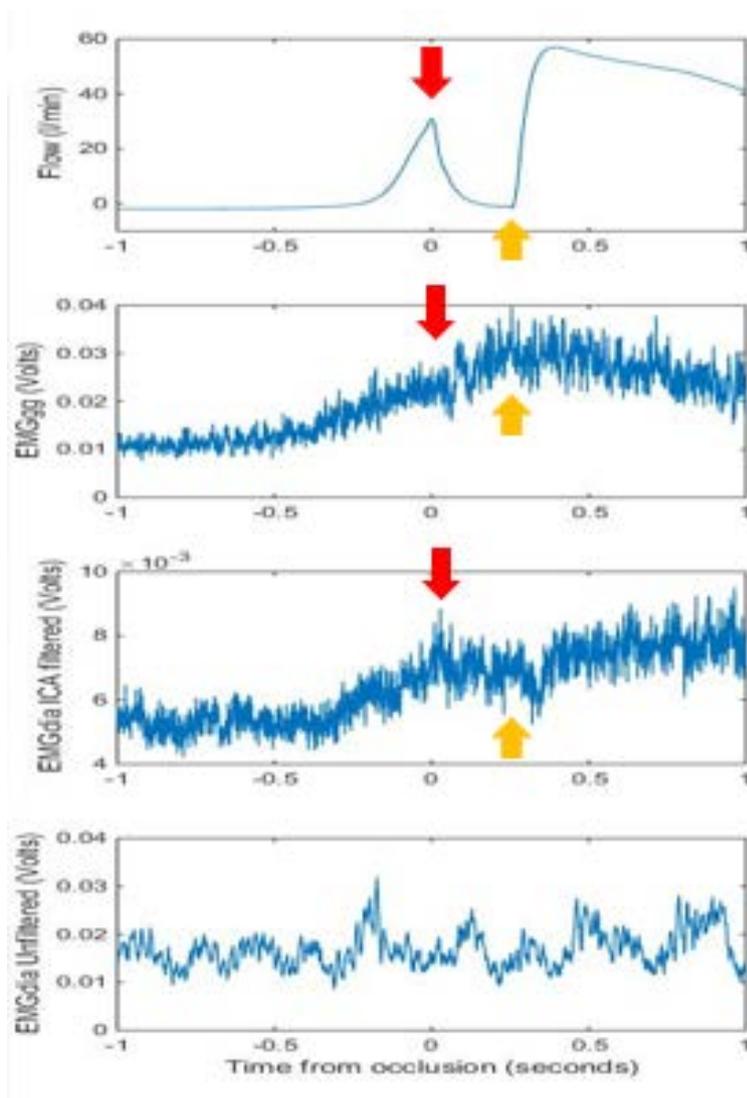
Figure 32 Cleaned EMGdi reflexes and EMGgg reflexes elicited by sudden airway occlusion

6.3 Discussion

The ICA-Wavelet filter has been tested and appears to be very useful for denoising EMGdi to reveal underlying inspiratory activity and reflex responses to airway occlusion.

Chapter 7. Conclusion

In conclusion, this thesis established a novel ICA-Wavelet denoising filter which has been successfully used in the study of respiratory reflex mediated changes in muscle electrical activity. Several experiments including ICA-Wavelet testing, performance evaluation and ICA-Wavelet optimization were designed to explore algorithm performance. 5-channel

signals were filtered and the result showed that ICA-Wavelet filter can efficiently remove ECG noise and relatively preserve underlying respiratory activity within the EMGdi signal. The median frequency after ICA-Wavelet filtering converged away from the main frequency range expected of ECG towards that expected for EMGdi. Overall power of the EMGdi signal also dropped with a dominated frequency peak about 0-40 Hz consistent with cardiac activity becoming significantly reduced. Comparsons of different wavelet basis in the db wavelet family, suggested there was not much difference on the EMGdi filtering performance. RMS and median frequency also suggested that the ICA-Wavelet filter is relatively robust to basis function choice within the db wavelet family. Validation of filtering output is inherently difficult since it is not possible to quantify real EMG signal versus the remaining amount of ECG artefact in real signals. Performance on simulated signals can be helpful, but simulated signals can only approximate real-world signals so we elected instead to focus on real signals collected during experimental paradigms where we expected that underlying EMGdi features should emerge following successful denoising. Visual inspection of pre- vs post-filtered signals as well as evidence from RMS, mean frequencies/spectrum comparisonssupport the utility of the ICA approach. We also tested the filter using another group of clinical data. The result showed that this technique is suitable for general EMGdi data although some parameters such as threshold value could be adjusted for different condition.

The signal averaged airfow, rectified raw EMGdi responses, rectified filtered EMGdi responses and EMGgg responses to the sudden airway occlusion were collected to present response features and test the performance of the filter. The results showed that denoised EMGdi appeared to reveal both inspiratory activation and short-latency reflex responses expected to emerge in the presence of successful denoising. This overall pattern of inspiratory EMGdi activity appeared to be very similar to that of simultaneously recorded EMGgg uncontaminated by ECG. These very promising initial data support that further work with more participants to examine EMGgg vs EMGdi responses in more detail.

Chapter 8. Appendix

7.1 Code for ICA-Wavelet algorithm
function ICA_Wavelet_main

```matlab
clear;clc;close all;

load ('new_neura.mat')

raw=neura(:,:);

% load slp;  raw=slp;

figure(1);

winrect=[200,200,540,400];%[distance left bottom length height]

set(gcf,'position',winrect)

set(gca,'box','on','fontname','Calibri','fontsize',9)

% hold on; title('raw')

wplot(raw);

% ylabel('Amplitude [mV]','fontname','Calibri','fontsize',9);

xlabel('Time [sec]','fontname','Calibri','fontsize',9);

% hold off;

%%%%%%%%%%%%%%%%%%%%%%%%%%%%%%%%%%%%%%%%%%%

[y,v,w]=fastICA(raw);

%%%%%%%%%%%%%%%%%%%%%%%%%%%%%%%%%%%%%%%%%%%%

figure(2);

title('ICs')

mplot(y);

%%%%%%%%%%%%%%%%%%%%%%%%%%%%%%%%%%%%%%%%%%%

y(1,:)=0;

%%%%%%%%%%%%%%%%%%%%%%%%%%%%%%%%%%%%%%%%%%%%

for i=2:size(raw,1)-1

    y(i+1,:)=wavewu(y(i+1,:));

end

emgdi_wu=inv(v)*w'*y;

% save('neura_channel1.mat','emgdi_wu');
```

```matlab
%%%%%%%%%%%%%%%%%%%%%%%%%%%%%%%%%%%%%%%%%%%%%%
figure(3);

title('Results')

wplot(emgdi_wu);

function [y,v,w]=fastICA(x)

tic; %Start a stopwatch timer.

[r,c]=size(x);%r=8;c=24121

x=x-mean(x')'*ones(1,c);

[E,D]=eig(cov(x',1));

v=E*(D^(-0.5))*E';

z=v*x;

epsilon=1e-6;

m=r;

w=zeros(r,1);

for p=1:m

 w(:,p)=ones(r,1);

 w(:,p)=w(:,p)/norm(w(:,p));

 exit=0;

 count=0;

 iter=1;

while exit==0

count=count+1;

temp=w(:,p);

 for i=1:m

    w(i,p)=mean(z(i,:).*tanh(temp'*z))-(mean(1-(tanh(temp'*z).^2)).*temp(i,1));

 end

 ssum=zeros(r,1);
```

```matlab
    for counter=1:p-1

        ssum=ssum+(w(:,p)'*w(:,counter))*w(:,counter);

    end

  w(:,p)=w(:,p)-ssum;

  w(:,p)=w(:,p)/norm(w(:,p));

  if(abs((dot(w(:,p),temp)))<1+epsilon)&(abs((dot(w(:,p),temp)))>1-epsilon)

      exit=1;

  end

  iter=iter+1;

  end

end

w=w';

%[m,in]=sort(power);

%w=w(in,:);

y=w*z;

toc;

 function emg=wavewu(emgdi)

% load slp; emgdi=slp(size(slp,1),:);

ls = length(emgdi); %find length the vector

f=(1:ls)/2000;

dc = [];

[c,l] = wavedec(emgdi,5,'db1'); % decomposed.c:coefficient l:length

figure;

subplot(2,1,1);

plot(f,emgdi,'b');%title('Original signal');

xlabel('(a)');

ylabel('Amp(V)');
```

```matlab
axis([0 ls/2000 -500 500]);


upbound = 15;

lowbound = 8;

step = upbound - lowbound;


ca5 = [];

ca5 = c(1:l(1));


num = l(1);

n = 1;

th=[2 2 3 4 5 5];

% th=5*ones(1,6);

k=[];

for i = 1:upbound*n

    ave = sum(abs(ca5((i+lowbound*n):(i+upbound*n-n))))/step*n;

    k(i) = abs(ca5(i))/ave;

    if k(i) >= th(1)

        ca5(i) = 0;

    end

end


for i = (num-upbound*n+1):num

    ave = sum(abs(ca5((i-upbound*n+n):(i-lowbound*n))))/step*n;

    k(i) = abs(ca5(i))/ave;

    if k(i) >= th(1)

        ca5(i) = 0;
```

```
      end
end
for i = upbound*n:(num-upbound*n)
   ave = (sum(abs(ca5((i-upbound*n+n):(i-lowbound*n))))  +
sum(abs(ca5((i+lowbound*n):(i+upbound*n-n)))))/(2*step*n);
   k(i) = abs(ca5(i))/ave;
   if k(i) >= th(1)
      ca5(i) = 0;
   else
   end
end
dc(1:l(1)) = ca5;


cd5 = [];
cd5 = c((1+l(1)):(l(1)+l(2)));
%hold on
num = l(2);
n = 1;


k=[];
for i = 1:(upbound*n-1)
   ave = sum(abs(cd5((i+lowbound*n):(i+upbound*n-n))))/step*n;
   k(i) = abs(cd5(i))/ave;
   if k(i) >= th(2)
      cd5(i) = 0;
   end
end
for i = (num-upbound*n+1):num
```

```
    ave = sum(abs(cd5((i-upbound*n+n):(i-lowbound*n))))/step*n;

    k(i) = abs(cd5(i))/ave;

    if k(i) >= th(2)

        cd5(i) = 0;

    end

end


for i = upbound*n:(num-upbound*n)

    ave = (sum(abs(cd5((i-upbound*n+n):(i-lowbound*n))))   +
sum(abs(ca5((i+lowbound*n):(i+upbound*n-n)))))/(2*step*n);

    k(i) = abs(cd5(i))/ave;


    if k(i) >= th(2)

        cd5(i) = 0;

    else

    end

end


dc((1+l(1)):(l(1)+l(2)))  = cd5;



%%%%%%%%%%%%%%%%%%%%%%%%%%%%%%%%%%%%%%%%%%%%%%%%%%%%%%%%
%%%%%%%%%%%%%%%%%%%%%%%%%%%%%%%%%%%%%%%%%%%%%%%%

cd4 = c(1+l(1)+l(2):l(1)+l(2)+l(3));

ca5 = [];

ca5 = cd4;

%hold on

num = l(3);
```

```matlab
n = 2;

k=[];

for i = 1:(upbound*n-1)

  ave = sum(abs(ca5((i+lowbound*n):(i+upbound*n-n))))/step*n;

  k(i) = abs(ca5(i))/ave;

  if k(i) >= th(3)

    ca5(i) = 0;

  end

end

for i = (num-upbound*n+1):num

  ave = sum(abs(ca5((i-upbound*n+n):(i-lowbound*n))))/step*n;

  k(i) = abs(ca5(i))/ave;

  if k(i) >= th(3)

    ca5(i) = 0;

  end

end

for i = upbound*n:(num-upbound*n)

  ave = (sum(abs(ca5((i-upbound*n+n):(i-lowbound*n))))  +
sum(abs(ca5((i+lowbound*n):(i+upbound*n-n)))))/(2*step*n);

  k(i) = abs(ca5(i))/ave;

  if k(i) >= th(3)

    ca5(i) = 0;

  else

  end

end
```

```matlab
dc(1+l(1)+l(2):l(1)+l(2)+l(3)) = ca5;




%%%%%%%%%%%%%%%%%%%%%%%%%%%%%%%%%%%%%%%%%%%%%%%%%%%%
%%%%%%%%%%%%%%%%%%%%%%%%%%%%%%%%%%%%%%%%%%%

cd3 = c(1+l(1)+l(2)+l(3):l(1)+l(2)+l(3)+l(4));

ca5 = [];

ca5 = cd3;

%hold on

num = l(4);

n = 4;


k=[];


for i = 1:(upbound*n-1)

    ave = sum(abs(ca5((i+lowbound*n):(i+upbound*n-n))))/step*n;

    k(i) = abs(ca5(i))/ave;

    if k(i) >= th(4)

        ca5(i) = 0;

    end

end

for i = (num-upbound*n+1):num

    ave = sum(abs(ca5((i-upbound*n+n):(i-lowbound*n))))/step*n;

    k(i) = abs(ca5(i))/ave;

    if k(i) >= th(4)

        ca5(i) = 0;
```

```matlab
    end

end


for i = upbound*n:(num-upbound*n)

   ave = (sum(abs(ca5((i-upbound*n+n):(i-lowbound*n))))  +
sum(abs(ca5((i+lowbound*n):(i+upbound*n-n)))))/(2*step*n);

   k(i) = abs(ca5(i))/ave;


   if k(i) >= th(4)

      % author: wfy@nwpu.edu.cn

      ca5(i) = 0;

   else

   end

end


dc(1+l(1)+l(2)+l(3):l(1)+l(2)+l(3)+l(4))  = ca5;




%%%%%%%%%%%%%%%%%%%%%%%%%%%%%%%%%%%%%%%%%%%%%%%%%%%%%%%%%%%%%%
%%%%%%%%%%%%%%%%%%%%%%%%%%%%%%%%%%%%%%%%%%%%%%%%%

cd2 = c(1+l(1)+l(2)+l(3)+l(4):l(1)+l(2)+l(3)+l(4)+l(5));

ca5 = [];

ca5 = cd2;

%hold on

num = l(5);

n = 8;


k=[];
```

```matlab
for i = 1:(upbound*n-1)

    ave = sum(abs(ca5((i+lowbound*n):(i+upbound*n-n))))/step*n;

    k(i) = abs(ca5(i))/ave;

    if k(i) >= th(5)

        ca5(i) = 0;

    end

end

for i = (num-upbound*n+1):num

    ave = sum(abs(ca5((i-upbound*n+n):(i-lowbound*n))))/step*n;

    k(i) = abs(ca5(i))/ave;

    if k(i) >= th(5)

        ca5(i) = 0;

    end

end


for i = upbound*n:(num-upbound*n)

    ave = (sum(abs(ca5((i-upbound*n+n):(i-lowbound*n))))  +
sum(abs(ca5((i+lowbound*n):(i+upbound*n-n)))))/(2*step*n);

    k(i) = abs(ca5(i))/ave;


    if k(i) >= th(5)

        ca5(i) = 0;

    else

    end

end


dc(1+l(1)+l(2)+l(3)+l(4):l(1)+l(2)+l(3)+l(4)+l(5))  = ca5;
```

```
%%%%%%%%%%%%%%%%%%%%%%%%%%%%%%%%%%%%%%%%%%%%%%%%%%%%%%%%%%%
%%%%%%%%%%%%%%%%%%%%%%%%%%%%%%%%%%%%%%%%%%%%%%

%figure(6)

cd1 = c(1+l(1)+l(2)+l(3)+l(4)+l(5):l(1)+l(2)+l(3)+l(4)+l(5)+l(6));

ca5 = [];

ca5 = cd1;

%hold on

num = l(6);

n = 16;


k=[];


for i = 1:(upbound*n-1)

    ave = sum(abs(ca5((i+lowbound*n):(i+upbound*n-n))))/step*n;

    k(i) = abs(ca5(i))/ave;

    if k(i) >= th(6)

        ca5(i) = 0;

    end

end

for i = (num-upbound*n+1):num

    ave = sum(abs(ca5((i-upbound*n+n):(i-lowbound*n))))/step*n;

    k(i) = abs(ca5(i))/ave;

    if k(i) >= th(6)

        ca5(i) = 0;

    end

end
```

```matlab
for i = upbound*n:(num-upbound*n)

    ave = (sum(abs(ca5((i-upbound*n+n):(i-lowbound*n))))  +
sum(abs(ca5((i+lowbound*n):(i+upbound*n-n)))))/(2*step*n);

    k(i) = abs(ca5(i))/ave;


    if k(i) >= th(6)

        ca5(i) = 0;

    else

    end

end


dc(1+l(1)+l(2)+l(3)+l(4)+l(5):l(1)+l(2)+l(3)+l(4)+l(5)+l(6))  = ca5;




%%%%%%%%%%%%%%%%%%%%%%%%%%%%%%%%%%%%%%%%%%%%%%%%%%%%%%%%%%%%
%%%%%%%%%%%%%%%%%%%%%%%%%%%%%%%%%%%%

emg = waverec(dc,l,'db1'); %wavelet reconstruction

subplot(2,1,2);

plot(f,emg,'r');

%title('Processed signal');

xlabel('(b)');

ylabel('Amp(V)');

axis([0 ls/2000 -500 500]);

return

function mplot(x)

[dim,sample]=size(x);

if dim>sample x=x';
```

```matlab
[dim,sample]=size(x);

end

if dim>10

error ('dim can not more than ten');

end

t=0:0.0005:(sample-1)*0.0005;


winrect=[200,200,540,400];

%[distance left bottom length height]

set(gcf,'position',winrect);

set(gca,'box','on','fontname','Calibri','fontsize',9);

hold on;

for i=1:dim

    subplot(dim,1,i);

    plot(t,x(i,:),'k');

    ylabel('Amplitude [dV]','fontname','Calibri','fontsize',9);

    xlabel('Time [sec]','fontname','Calibri','fontsize',9);

    axis([0 sample*0.0005 min(x(i,:)) max(x(i,:))]);

%   axis('tight');

end

function wplot(x)

[dim,sample]=size(x);

if dim>sample x=x';

[dim,sample]=size(x);

end

t=0:0.0005:(sample-1)*0.0005;

if dim>10
```

error ('dim can not more than ten');

end

for i=1:dim

   subplot(dim,1,i);

   plot(t,x(i,:),'k');

   axis([0 sample*0.0005 -10 10]);

   ylabel(['(',num2str(i),')']);

end

ylabel('Amplitude/mV','fontname','Calibri','fontsize',9);

xlabel('Time/s','fontname','Calibri','fontsize',9);

7.2 Code for SNR, RMS and Fmid

```matlab
%% RMS & SNR

function y=RMS(x)
clear;clc;close all;
load('dia.mat')
load('clean_db1.mat')
s1=raw(:,1)';%noise signal
s2=emgdi_wu(1,:);%cleaned signal

% [p1,w1]=pwelch(s1);
% sp1=size(p1);
% sw1=size(w1);
% M_orig=sum(p1.*w1);
%
% [p2,w2]=pwelch(s2);
% sp2=size(p2);
% sw2=size(w2);
% M=sum(p2.*w2);
rms_o=sqrt(sum(s1.^2)/size(s1,1))
rms_d=sqrt(sum(s2.^2)/size(s2,1))
snr_db=20*log10(rms_d/(rms_o-rms_d));
snr_lin=10^(snr_db/20);
% rms_ICA=sqrt(M/length(p2))
```

7.3 Code for 'pre filter'

```matlab
% function filter = Hfilter(raw)
fs=1000;%sample rate
dt=1/2*fs;

load ('neura data.mat')
%%
%channel one high pass filter

N=length(raw1);
```

```matlab
t=(0:N-1)*dt;
data_fft=fft(raw1);
df=(2*fs)/N;
data_f=(0:N-1)*df;
xlim([0,250]);

id0=find(data_f<10);%apply 10 Hz high pass filter
id0_len=length(id0);
data_fft(id0)=0;
data_fft(((end+1)-(id0_len-1)):end)=0;
data_ifft1=real(ifft(data_fft));
%%
%channel two
raw2=raw(2,:);

N=length(raw2);

t=(0:N-1)*dt;
data_fft=fft(raw2);
df=(2*fs)/N;
data_f=(0:N-1)*df;
xlim([0,250]);

id0=find(data_f<10);
id0_len=length(id0);
data_fft(id0)=0;
data_fft(((end+1)-(id0_len-1)):end)=0;
data_ifft2=real(ifft(data_fft));
%%
%channel three
raw3=raw(3,:);

N=length(raw3);

t=(0:N-1)*dt;
data_fft=fft(raw3);
df=(2*fs)/N;
data_f=(0:N-1)*df;
xlim([0,250]);

id0=find(data_f<10);
id0_len=length(id0);
data_fft(id0)=0;
data_fft(((end+1)-(id0_len-1)):end)=0;
data_ifft3=real(ifft(data_fft));
%%
%channel 4
raw4=raw(4,:);

N=length(raw4);

t=(0:N-1)*dt;
data_fft=fft(raw4);
df=(2*fs)/N;
data_f=(0:N-1)*df;
xlim([0,250]);

id0=find(data_f<10);
```

```matlab
id0_len=length(id0);
data_fft(id0)=0;
data_fft(((end+1)-(id0_len-1)):end)=0;
data_ifft4=real(ifft(data_fft));
%%
%channel five
raw5=raw(5,:);

N=length(raw5);

t=(0:N-1)*dt;
data_fft=fft(raw5);
df=(2*fs)/N;
data_f=(0:N-1)*df;
xlim([0,250]);

id0=find(data_f<10);
id0_len=length(id0);
data_fft(id0)=0;
data_fft(((end+1)-(id0_len-1)):end)=0;
data_ifft5=real(ifft(data_fft));
%%
%plot
figure (1);
subplot(5,1,1)
plot(t,raw1,'k');
title('raw')
ylabel(['(',num2str(1),')']);
subplot(5,1,2)
plot(t,raw2,'k');
ylabel(['(',num2str(2),')']);
subplot(5,1,3)
plot(t,raw3,'k');
ylabel(['(',num2str(3),')']);
subplot(5,1,4)
plot(t,raw4,'k');
ylabel(['(',num2str(4),')']);
subplot(5,1,5)
plot(t,raw5,'k');
ylabel(['(',num2str(5),')']);

figure (2);
subplot(5,1,1)
plot(t,data_ifft1,'k');
title('High pass filtered')
ylabel(['(',num2str(1),')']);
subplot(5,1,2)
plot(t,data_ifft2,'k');
ylabel(['(',num2str(2),')']);
subplot(5,1,3)
plot(t,data_ifft3,'k');
ylabel(['(',num2str(3),')']);
subplot(5,1,4)
plot(t,data_ifft4,'k');
ylabel(['(',num2str(4),')']);
subplot(5,1,5)
plot(t,data_ifft5,'k');
ylabel(['(',num2str(5),')']);
```

```
%%
%combine channels
neura=[data_ifft1;data_ifft2;data_ifft3;data_ifft4;data_ifft5];
```

Chapter 8. References

Aapo, H, Erkki, O & Juha, K 2001, *Independent component analysis*, J. Wiley New York

Bartolo, A, Roberts, C, Dzwonczyk, RR & Goldman, E 1996, 'Analysis of diaphragm EMG signals: comparison of gating vs. subtraction for removal of ECG contamination', *Journal of Applied Physiology*, vol. 80, no. 6, pp. 1898-902.

Bates, JHT 1998, 'Linear Systems and the 1-D Fourier Transform', in TM Peters & J Williams (eds), *The Fourier Transform in Biomedical Engineering*, Birkhäuser Boston, Boston, MA, pp. 25-52.

Beck, J, Sinderby, C, Lindstrom, L & Grassino, A 1996, 'Influence of bipolar esophageal electrode positioning on measurements of human crural diaphragm electromyogram', *Journal of Applied Physiology*, vol. 81, no. 3, pp. 1434-49.

Carré, P, Leman, H, Fernandez, C & Marque, C 1998, 'Denoising of the uterine EHG by an undecimated wavelet transform', *IEEE transactions on biomedical engineering*, vol. 45, no. 9, pp. 1104-13.

Deny, Y, Wolf, W & Bullemer, F 1988, 'Time frequency analysis of diaphragmatic electromyogram for the detection of diaphragm fatigue', in *Engineering in Medicine and Biology Society, 1998. Proceedings of the 20th Annual International Conference of the IEEE*, vol. 6, pp. 3207-10.

Donoho, DL 1992, *Denoising by Soft-Thresholding," Dept. of Statistics*, Stanford University.

Eckert, DJ, McEvoy, RD, George, KE, Thomson, KJ & Catcheside, PG 2008, 'Effects of hypoxia on genioglossus and scalene reflex responses to brief

pulses of negative upper-airway pressure during wakefulness and sleep in healthy men', *Journal of Applied Physiology*, vol. 104, no. 5, pp. 1426-35.

Garg, G, Singh, V, Gupta, J & Mittal, A 2010, 'Optimal algorithm for ECG denoising using discrete wavelet transforms', in *Computational Intelligence and Computing Research (ICCIC), 2010 IEEE International Conference on*, pp. 1-4.

Gross, D, Grassino, A, Ross, WR & Macklem, PT 1979, 'Electromyogram pattern of diaphragmatic fatigue', *Journal of Applied Physiology*, vol. 46, no. 1, pp. 1-7.

He, C, Xing, JC & Yang, QL 2014, 'Optimal Wavelet Basis Selection for Wavelet Denoising of Structural Vibration Signal.', *Applied Mechanics and Materials*, no. 578-579, pp. 1059-63.

Horrobin, DF 1973, 'Circulation', in *An Introduction to Human Physiology*, Springer Netherlands, Dordrecht, pp. 105-18.

Hyvärinen, A, Karhunen, J & Oja, E 2004, *Independent component analysis*, vol. 46, John Wiley & Sons.

Hyviirinen, A 2001, 'Fast ICA by a fixed-point algorithm that maximizes non-Gaussianity', *Independent component analysis: principles and practice*, p. 71.

Johnson, DH 2006, 'Signal-to-noise ratio', *Scholarpedia*, vol. 1, no. 12, p. 2088.

Lake, FR, Finucane, KE & Hillman, DR 1999, 'Diaphragm inhibition with positive pressure ventilation: quantification of mechanical effects', *Respiration Physiology*, vol. 118, no. 2–3, pp. 149-61.

Levine, S, Gillen, J, Weiser, P, Gillen, M & Kwatny, E 1986, 'Description and validation of an ECG removal procedure for EMGdi power spectrum analysis', *Journal of Applied Physiology*, vol. 60, no. 3, pp. 1073-81.

Levine, S & Gillen, M 1987, 'Diaphragmatic pressure waveform can predict electromyographic signs of diaphragmatic fatigue', *Journal of Applied Physiology*, vol. 62, no. 4, pp. 1681-9.

Lu, J 2013, *Wavelet transform*, NBALab, viewed 21 March 2017, <http://www.ym.edu.tw/~cflu/CFLu_course_matlabsig.html>.

Luo, Y-MPT, Jing MB; Jolley, Caroline MD; Steier, Joerg MD; Zhong, Nan-Shan MD, FCCP; Moxham, John MD; Polkey, Michael Iain PhD 2009, 'Distinguishing Obstructive From Central Sleep Apnea Events*: Diaphragm Electromyogram and Esophageal Pressure Compared.', *Clinical Medicine*, pp. 1133-41.

Mallat, S 1999, *A wavelet tour of signal processing*, Academic press.

Mallat, S & Hwang, WL 1992, 'Singularity detection and processing with wavelets', *IEEE transactions on information theory*, vol. 38, no. 2, pp. 617-43.

Merletti, R, Sabbahi, MA & De Luca, CJ 1984, 'Median frequency of the myoelectric signal', *European journal of applied physiology and occupational physiology*, vol. 52, no. 3, pp. 258-65.

Oja, E & Yuan, Z 2006, 'The FastICA algorithm revisited: Convergence analysis', *IEEE Transactions on Neural Networks*, vol. 17, no. 6, pp. 1370-81.

Pathak, RS & Singh, A 2016, 'Distributional Wavelet Transform', *Proceedings of the National Academy of Sciences, India Section A: Physical Sciences*, vol. 86, no. 2, pp. 273-7.

Roussos, CS & Macklem, PT 1977, 'Diaphragmatic fatigue in man', *Journal of Applied Physiology*, vol. 43, no. 2, pp. 189-97.

Roy, SH, Bonato, P & Knaflitz, M 1998, 'EMG assessment of back muscle function during cyclical lifting', *Journal of Electromyography and Kinesiology*, vol. 8, no. 4, pp. 233-45.

Seljuq, U, Himayun, F & Rasheed, H 2014, 'Selection of an optimal mother wavelet basis function for ECG signal denoising', in *17th IEEE International Multi Topic Conference 2014*, pp. 26-30.

Semmlow, JL & Griffel, B 2014, *Biosignal and medical image processing*, CRC press.

Sinderby, CA, Beck, JC, Lindström, LH & Grassino, AE 1997, 'Enhancement of signal quality in esophageal recordings of diaphragm EMG', *Journal of Applied Physiology*, vol. 82, no. 4, pp. 1370-7.

Stadler, DL, McEvoy, RD, Bradley, J, Paul, D & Catcheside, PG 2010, 'Changes in lung volume and diaphragm muscle activity at sleep onset in obese obstructive sleep apnea patients vs. healthy-weight controls', *Journal of Applied Physiology*, vol. 109, no. 4, pp. 1027-36.

Tan, HR, Tan, A, Khong, P & Mok, V 2007, 'Best wavelet function identification system for ECG signal denoise applications', in *Intelligent and Advanced Systems, 2007. ICIAS 2007. International Conference on*, pp. 631-4.

Tan, J 2017, *AS WE LIVE & BREATHE – AN EFFECTIVE GUIDE ON BREATHING TO IMPROVE HEALTH & PERFORMANCE*, Genesis Gym, viewed 10 May 2017, <http://www.genesisgym.com.sg/live-breathe-effective-guide-breathing-improve-health-performance/>.

Wang, B, Kuruoglu, EE & Zhang, J 2009, 'ICA by Maximizing Non-stability', in T Adali, C Jutten, JMT Romano & AK Barros (eds), *Independent Component Analysis and Signal Separation: 8th International Conference, ICA 2009, Paraty, Brazil, March 15-18, 2009. Proceedings*, Springer Berlin Heidelberg, Berlin, Heidelberg, pp. 179-86.

West, JB 1990, *Physiological basis of medical practice*, Twelfth edition edn, USA.

Wu, F-Y, Tong, F & Yang, Z 2016, 'EMGdi signal enhancement based on ICA decomposition and wavelet transform', *Applied Soft Computing*, vol. 43, pp. 561-71.

Zhan, C, Yeung, LF & Yang, Z 2010, 'A wavelet-based adaptive filter for removing ECG interference in EMGdi signals', *Journal of Electromyography and Kinesiology*, vol. 20, no. 3, pp. 542-9.